Identification and characterization of a MAPT-targeting locked nucleic acid antisense oligonucleotide therapeutic for tauopathies

Amy Easton,[2,5,7] Marianne L. Jensen,[1,7] Congwei Wang,[3,7] Peter H. Hagedorn,[1] Yuwen Li,[2] Michael Weed,[2] Jere E. Meredith,[2] Valerie Guss,[2] Kelli Jones,[2] Martin Gill,[2] Carol Krause,[2] Jeffrey M. Brown,[2] Lisa Hunihan,[2] Joanne Natale,[2] Alda Fernandes,[2] Yifeng Lu,[2] Joe Polino,[2] Mark Bookbinder,[2] Greg Cadelina,[2] Yulia Benitex,[2] Ramola Sane,[2] John Morrison,[2] Dieter Drexler,[2] Stephen E. Mercer,[2] Charlotte Bon,[3] Nikhil J. Pandya,[3] Ravi Jagasia,[3] Tai-Hsien Ou Yang,[4] Tania Distler,[3] Fiona Grüninger,[3] Michael Meldgaard,[1] Marco Terrigno,[3] John E. Macor,[2] Charles F. Albright,[2] James Loy,[2] Anja M. Hoeg,[1] Richard E. Olson,[2] and Angela M. Cacace[2,6]

[1]Roche Pharma Research and Early Development, Therapeutic Modalities, Roche Innovation Center Copenhagen, Hørsholm DK 2970, Denmark; [2]Bristol Myers Squibb Research and Development, Cambridge, MA 02142, USA; [3]Roche Pharma Research and Early Development, Neuroscience and Rare Disease Discovery and Translational Area, Roche Innovation Center Basel, 4070 Basel, Switzerland; [4]Roche Pharma Research and Early Development, pREDi Data Science, Roche Innovation Center New York, Little Falls, NJ 07424, USA

Tau is a microtubule-associated protein (*MAPT*, tau) implicated in the pathogenesis of tauopathies, a spectrum of neurodegenerative disorders characterized by accumulation of hyperphosphorylated, aggregated tau. Because tau pathology can be distinct across diseases, a pragmatic therapeutic approach may be to intervene at the level of the tau transcript, as it makes no assumptions to mechanisms of tau toxicity. Here we performed a large library screen of locked-nucleic-acid (LNA)-modified antisense oligonucleotides (ASOs), where careful tiling of the *MAPT* locus resulted in the identification of hot spots for activity in the 3′ UTR. Further modifications to the LNA design resulted in the generation of ASO-001933, which selectively and potently reduces tau in primary cultures from hTau mice, monkey, and human neurons. ASO-001933 was well tolerated and produced a robust, long-lasting reduction in tau protein in both mouse and cynomolgus monkey brain. In monkey, tau protein reduction was maintained in brain for 20 weeks post injection and corresponded with tau protein reduction in the cerebrospinal fluid (CSF). Our results demonstrate that LNA-ASOs exhibit excellent drug-like properties and sustained efficacy likely translating to infrequent, intrathecal dosing in patients. These data further support the development of LNA-ASOs against tau for the treatment of tauopathies.

INTRODUCTION

The tau protein is a microtubule-associated protein (*MAPT*), initially thought to stabilize and regulate microtubule dynamics, that has since been implicated in a diverse set of signaling pathways and functions.[1,2] Tau protein is most abundantly expressed in neurons, but it is also found in other cell types, including oligodendrocytes and astrocytes.[3,4] Tau normally exists in a highly flexible, unstructured state and can interact not just with tubulin but with several binding partners, including other tau monomers.[5] In disease, tau becomes hyperphosphorylated, oligomerizes, and forms neurofibrillary tangles (NFTs), the neuropathological hallmark for a family of diseases called tauopathies.[6] Specifically, frontotemporal lobar degeneration (FTLD)-tau, can be caused by missense, silent, and intronic tau mutations[7,8] and progressive supranuclear palsy (PSP) can be caused by mutations in or near exon 10 or by tau polymorphisms comprising the H1 haplotype.[9,10] In Alzheimer's disease (AD) and FTLD-Tau, neurodegeneration is highly correlated with abnormal accumulation of insoluble, fibrillar tau.[11] Neurofibrillary tangles (NFTs) in AD develop in a distinct spatial pattern originating in the entorhinal cortex and then appearing later in hippocampus, neocortex, and the rest of the brain.[11,12] This temporospatial appearance of NFTs may be due to pathological forms of tau seeding new pathology through cell-to-cell spread.[13–16] Additionally, misfolded tau can sequester other soluble components such as spliceosomal proteins and Smad proteins, leading to disruptions of normal cellular function and neuronal loss.[17,18] Apart from a toxic gain-of-function mechanism, endogenous wild-type tau may promote or facilitate pathogenic processes in neurons, recently reviewed in detail.[2]

Not surprisingly, there is a strong interest to develop tau therapeutics across academia and industry. Therapeutic strategies have

encompassed a wide range of approaches, including the development of small molecules to inhibit tau acetylation, phosphorylation, or aggregation, and, more recently, development of large molecules to block the spread of tau.[19] Because the form of pathological tau differs across tauopathies, therapies agnostic to phosphorylation or aggregation state may have therapeutic benefit in all of these diseases. Antisense oligonucleotide (ASO) therapeutics offer such an approach and have been used successfully to treat peripheral and CNS diseases. The first clinical trial of an oligonucleotide directed to tau, IONIS-MAPTRx (BIIB080), is on-going in patients with mild AD.[20] The molecule contains a phosphorothioate backbone and incorporates a modification to the sugar ring with a 2'O-methoxyethyl (2'-MOE) in the flanks. Preclinical studies with similar tool ASOs demonstrated that tau transcript lowering was protective against pharmacological-induced seizure in mice as well as in reducing phosphorylated, aggregated tau and neurodegeneration.[21,22] Efficacy was observed even when ASO treatment was given after tau aggregation had begun, suggesting that this therapeutic approach might be used even after pathology develops and clinical diagnosis is confirmed in patients.[22]

Locked-nucleic-acid (LNA)-modified ASOs are well known for their improved affinity for target RNA,[23] which may translate into clinically relevant improvement over earlier generations of chemistry such as 2'-MOEs. Because oligonucleotides do not cross the blood-brain barrier, identification of potent molecules with long duration of action is important for minimizing intrathecal dose and dosing frequency in patients. Here, we present an *in vitro* to *in vivo* screening strategy in which we identified optimized tau-targeting LNA-ASOs. ASO-001933 has excellent *in vitro* and *in vivo* potency and selectivity, and is well tolerated in mice and monkeys. Remarkably, intrathecal delivery of ASO-001933 produced a long-lasting reduction of tau protein in brain and cerebrospinal fluid (CSF) of monkeys out to 20 weeks after treatment, suggesting potential for less frequent dosing in patients. Our data demonstrate the benefits of incorporating LNA chemistry into oligonucleotide therapeutics compared with other ASO chemistries.[22-25]

RESULTS

Initial tiling screen identified a parental ASO targeting the 3′ UTR of *MAPT* with high cross-species reactivity

To identify a specific, safe, and efficacious ASO targeting the human *MAPT* transcript, we applied a two-step strategy: first, an ASO-tiling screen to identify parental ASO, and, second, ASO optimization by varying LNA content and pattern. In the tiling screen, LNA gapmers were tiled along *MAPT* pre-mRNA, which included all exonic, intronic, and UTR sequences (Figure 1A). These gapmers were designed to perfectly match both human and cynomolgus (Cyno) monkey (*Macaca fascicularis*) *MAPT* transcripts and to have few to no predicted off-target effects based on a single base pair mismatch to other transcripts. To obtain gapmers with high affinity for *MAPT*, and to be able to recruit ribonuclease H (RNase H) for efficient target cleavage, ASOs between 14 and 20 nt in length were designed with three LNA moieties in each end flanking a stretch of 8–14 DNA moieties in the center. A total of 836 ASOs were screened for *in vitro* efficacy and toxicity. Mouse primary neuronal cultures, taken from

transgenic mice expressing the human *MAPT* gene,[26] were treated with the ASOs for 13 days and tau protein was measured using immunohistochemistry and high-content imaging. Efficacious LNA RNase H gapmer activity was defined as the ability to reduce tau protein more than 80%, and 661 ASOs of the total set of 836 were efficacious. Two *in vitro* toxicity neuronal assays were applied in the screening cascade. First, β-III tubulin protein levels were used for normalization in the high-content imaging assay but also as a measure of *in vitro* toxicity. Low toxicity in this assay was defined as less than 30% β-III tubulin content reduction. Second, changes in α-amino-3-hydroxy-5-methyl-4-isoxazolepropionic acid (AMPA)- mediated calcium oscillations were measured by live imaging.[27] A cutoff of less than 25% decrease of AMPA calcium oscillations compared with saline-treated cells was applied (Figures 1A and 1B). Sixty ASOs fulfilled all three criteria based on both *in vitro* activity and tolerability. Thirteen were further assessed for acute behavioral *in vivo* tolerability and tau mRNA reduction in a human tau (hTau) mouse model (Figure 1C). A dose of 100 μg of each ASO was injected intracerebroventricularly (ICV) and mice were sacrificed 72 h later. MAPT mRNA level in brain tissue was measured by qRT-PCR. Among all tested candidates, ASO-000013 was well tolerated and resulted in a significant tau transcript knockdown of 72%.

Alternative splicing and alternative polyadenylation of the *MAPT* gene generates six tau protein coding isoforms with two 3′ UTR isoforms (Figure 1D). ASO-000013 targets the long 3′ UTR isoform of *MAPT* pre-mRNA, which is the major isoform expressed in human frontal cortex.[28] The target sequence (138888–138903) is highly conserved across human, monkey, mouse, and rat. Taken together, ASO-000013 was chosen for further optimization (Table 1).

LNA pattern modifications on the parental sequence identified ASO-001933 as a potent *MAPT*-targeting ASO

The LNA patterns can lead to differences in ASO properties, including stability, toxicity and potency.[29,30] To optimize the design of our parental ASO, we synthesized 49 gapmers with varying numbers of LNA nucleosides and assessed their potency and tolerability in hTau mouse primary neuronal cultures. As depicted in the x axis of Figure 2A, the 20mer ASO sub-library contained three to 11 LNA nucleosides with different design patterns, both classical gapmers and also gapmers with reduced gap length due to introduction of an LNA in the gap. Tolerability was evaluated as described above for the tiling approach, and full concentration response curves were generated to inform *in vitro* potency represented by half maximal inhibitory concentration (IC_{50}) values. Most ASOs showed potencies in the 10–100 nM range as seen in Figure 2A and as exemplified for ASO-001933 (IC_{50} = 21.5nM) in Figure 2B. Despite good *in vitro* activity and tolerability, some oligos were not considered due to undesirable off-target effects on the ras homolog family member A gene (RhoA mRNA) (L.H. and J.N., data not shown). The 12 most active and tolerated candidates were selected for further *in vivo* evaluation (Figure 2A). Mice treated with 100 μg of ASO-001933 ICV showed robust tau mRNA reduction by 80% 72 h post dosing and no obvious acute *in vivo* signs as indicated by a tolerability scores of <1 in
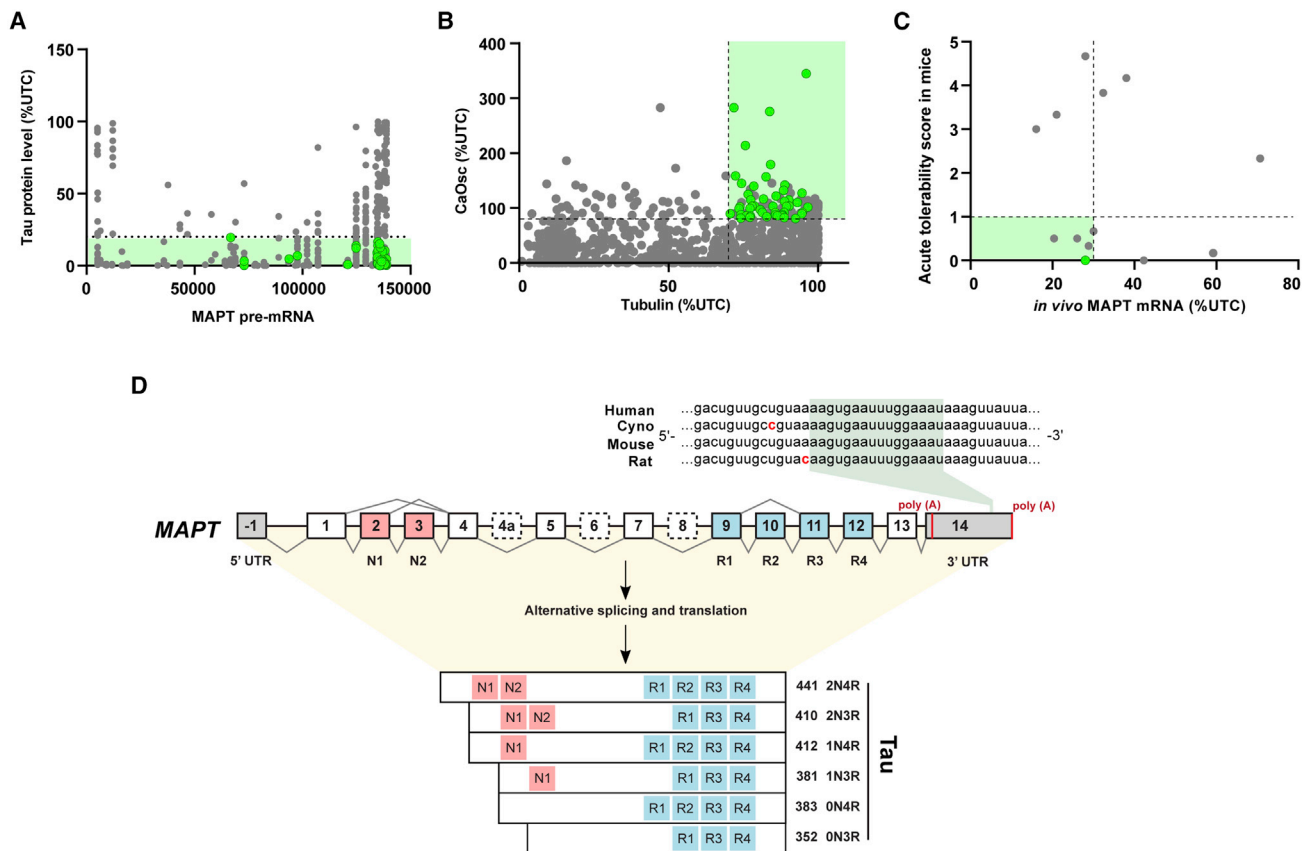
Figure 1. Initial screen identified parental *MAPT*-targeting sequence ASO-000013

(A and B) *In vitro* ASO-tiling and toxicity screen using hTau mouse primary neuronal cultures. Quantitative analysis of Tau protein levels after ASO treatments. ASO-targeting sites along *MAPT* transcript are shown on the x axis (A). Calcium oscillations (CaOsc) and β-III tubulin levels were evaluated for all ASOs used in tiling experiment (B). Each spot represents an ASO. Forty-seven ASOs (shown in green) showed low *in vitro* toxicity (tubulin >70% UTC and CaOsc >75% UTC) and good target knockdown efficiency (>80% UTC, B). (C) Thirteen out of 47 ASOs were selected for further evaluation using hTau mice. Assessment of *in vivo* acute tolerability and relative *MAPT* expression for each selected ASO. Each spot represents an ASO. ASO (shown in green) was selected as a parental *MAPT*-targeting sequence ASO-000013. (D) Alternative splicing of the MAPT gene generates six tau isoforms, named after the number of N-terminal repeats (0 N, 1 N, and 2 N) and C-terminal microtubule-binding domain repeats (3R and 4R). The first two exons (−1, 1) encode the 5′ untranslated region (UTR) and exon 14 encodes the 3′ UTR. The exons 4a, 6, and 8 are only part of the mature tau transcript in the peripheral nervous system. The target RNA sequence of ASO-000013 in exon 14 of tau mRNA is highlighted in green. The surrounding sequence in human, Cyno monkey, mouse, and rat show high conservation across different species. Nucleotides in red differ from the human sequence.

a modified Irwin battery[31] (Figure 2C). Considering selectivity, *in vitro* potency, and tolerability, as well as *in vivo* activity and tolerability measures, ASO-001933 was selected as lead ASO and further characterized *in vitro* and *in vivo*.

ASO-001933 potently and selectively reduced tau protein in human neurons

The potency of ASO-001933 was evaluated in dose-response experiments in human embryonic stem cell (hESC)-derived neuronal cultures. The neuronal cultures were treated with ASO-001933 or non-targeting (NT) control gapmer at various doses from day 0 of neuronal differentiation (Figure 3A). After 42 days of treatment, mRNA and protein levels were quantified by qRT-PCR and AlphaLISA, respectively. Our lead ASO clearly demonstrated a dose-dependent reduction of tau mRNA with an absolute IC_{50} value of 9.79 nM, and tau protein

was also dose dependently reduced with an absolute IC_{50} value of 12.62 nM as well as phospho-Tau with an absolute IC_{50} value 6.82 nM. In comparison, BIIB080 had 3- to 5-fold less activity in human neurons (Figure 3B). In addition, no evidence of neuronal toxicity was observed for cultures treated to 5 μM, an almost 500 times higher concentration than the IC_{50} values (Figure S1). Consistent with our AlphaLISA data, tau protein was lowered dramatically, as shown by immunoblot following 1 μM ASO-001933 treatment (Figure S2).

Our RNA sequencing (RNA-seq) data suggest that both 3R and 4R tau isoforms are expressed in the hESC-derived neuronal model and were reduced by at least 70% upon ASO-001933 treatment (Figures S3 and 3C). To evaluate the knockdown efficiency of ASO-001933 on mature neurons, we conducted a 2-week treatment on fully differentiated neurons (DIV29 to DIV 42), which resulted in a 90% RNA reduction and

Table 1. Details of oligonucleotide sequences

ID	Sequence	Sequence nt length	Pre-mRNA start	Pre-mRNA end	Pre-mRNA CDS UTR	Pre-mRNA int Exn
ASO-000013	ATTtccaaattcaCTT	16	133968	133983	UTR3	EXN14
ASO-001933	AtTTCcaaattcactTTtAC	20	133964	133983	UTR3	EXN14
NT ASO	CcAAAtcttataataACtAC	20	N/A	N/A	N/A	N/A

For MAPT sequence, see RefSeqGene record NG_007398.1.

30% protein reduction (Figure S4). To visualize tau reduction *in situ*, RNA fluorescent *in situ* hybridization (FISH) and immunocytochemistry (ICC) were performed on cells incubated with 1 μM ASO-001933. In FISH, two sets of probes were applied to target *MAPT* long 3′ UTR and CDS respectively. Consistent with previous findings, RNA FISH results suggest that *MAPT* with long 3′ UTR is the major isoform in human neurons, and ASO-001933 was able to efficiently reduce its FISH signal as well as tau protein staining (Figures 3D and 3E). Similar efficient tau knockdown was observed for tau protein in Cyno induced pluripotent stem cell (iPSC)-derived neurons (Figure S6).

To investigate transcriptomic and proteomic changes after long-term ASO-001933 treatment, we performed RNA profiling by RNA-seq and protein profiling by mass spectrometry (MS) on human neurons treated for 6 weeks. At the RNA level, four genes (*MAPT*, *LOC107987009*, *LOC107986994*, *LINGO2*) were differentially expressed upon 1 μM ASO-001933 treatment, among which tau exhibited the greatest decrease (log2FC = −2.7) in comparison with the NT control (Figure S5). However, among these genes, tau is the only one showing significant reduction at the protein level (log2FC = −2.94) (Figure 3F and Table S1). To assess the off-targets of ASO-001933, we conducted an acute treatment on human neurons at 5 μM for 72 h. Our RNA-seq data revealed that MAPT is the only differentially regulated gene (log2FC = −1.86) (Figure 3G). Interestingly, experimental selectivity for ASO-001933 was similar to predicted selectivity of this molecule (Table S2). These results suggest that our lead tau-directed oligo was optimized for potency and selectivity at both the RNA and protein level.

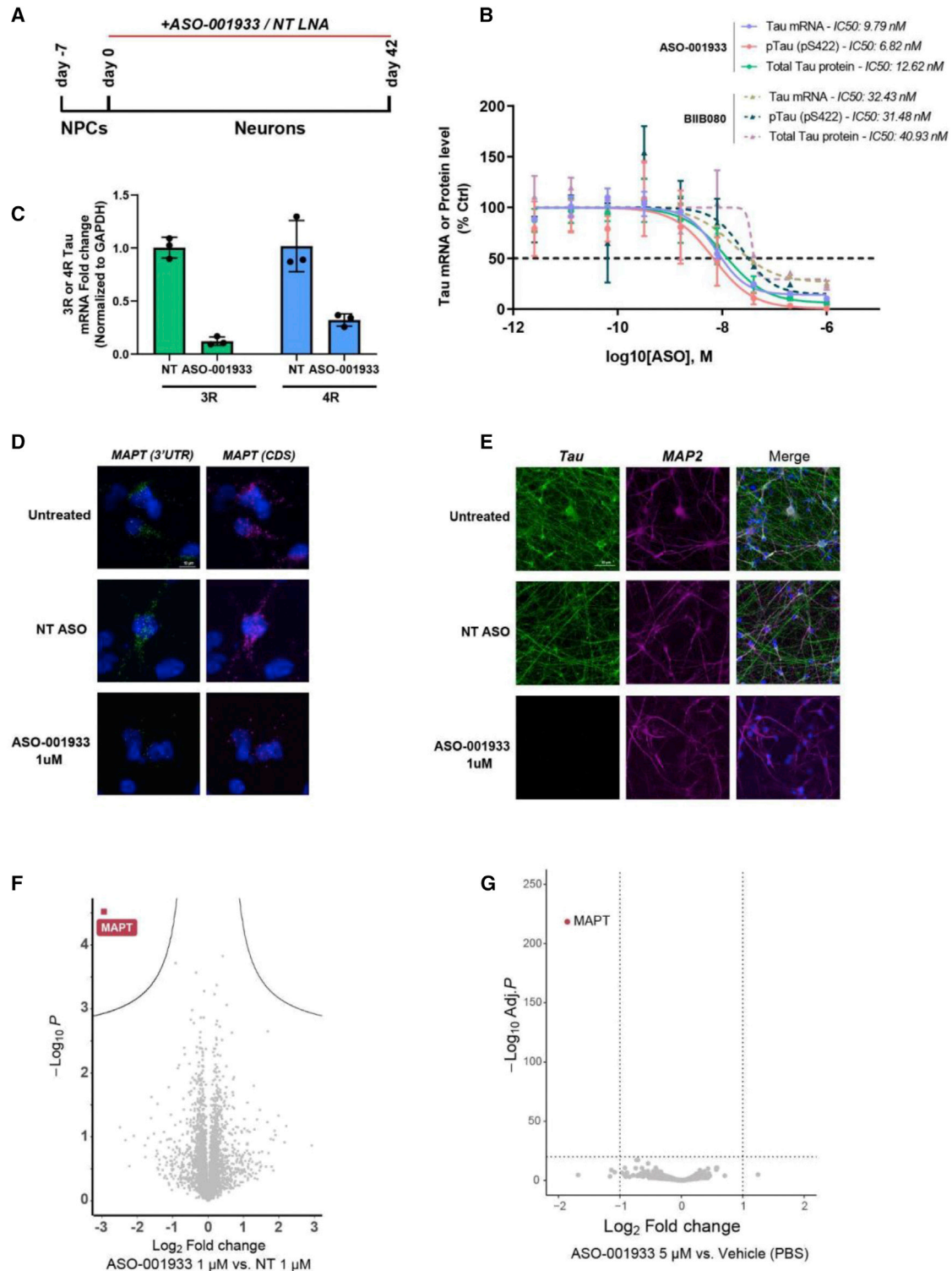### ASO-001933 potently reduced tau mRNA and protein in mice

C57Bl/6J mice given a single injection of 100 μg of ASO-001933 delivered into the right lateral ventricle resulted in transcript lowering with a peak of 58% tau mRNA reduction in cortex by 2 weeks post injection (n = 10–20/group; Figure 4A). Interestingly, tau protein levels lagged behind the changes in transcript, with peak lowering of 55% detected at 8 weeks post dose. Tau protein levels were still reduced, while transcript had partially returned to baseline levels. This observation fits with a longer *in vivo* half-life for the tau protein.[32] Knockdown corresponded well with ASO concentrations in the brain. Brain levels of ASO were close to 1 μM at 3 days after the injection and were barely detectable by 20 weeks post injection (Figure 4A). In this study, animals were weighed weekly to monitor body weight and general health. No gross side effects were observed, and ASO-0001933 mice gained weight throughout the 20-week time frame, similar to saline-treated mice (Figure S8A). ASO-001933 dose-response studies

were conducted at several time points, demonstrating dose-dependent knockdown of tau mRNA (one-way ANOVA, F = 77.2, p < 0.0001; Dunnett's post hoc, p < 0.0001; Figure 4B) and even greater reduction of tau protein at 8 weeks following a single dose (one-way ANOVA, F = 108.6, p < 0.0001; Dunnett's post hoc, p < 0.0001; Figure 4C). A PK/PD model was derived to link brain exposure to mRNA and protein knockdown (Figure S9). The mRNA half-life was found to be close to 3 days, while the protein half-life was about 10 days. To maintain the protein lowering of 50%, a dosing regimen of 100 μg every 10 weeks or 200 μg every 16 weeks can be selected (Figure 7A). ASO-001933 was also tested for activity on the human *MAPT* transcript in hTau mice[26] on a mouse tau knockout background. A single dose of 100 μg of ICV resulted in a 56% tau mRNA reduction 1 week post dose (one-way ANOVA, F = 15.9, p < 0.0001; Dunnett's post hoc versus saline, p < 0.05, p < 0.01, p < 0.0001; Figure 4D). Protein lowering was not yet detected at this time point, similar to what was observed in C57Bl/6J mice. A subsequent dose-response study conducted in mice expressing both human and mouse MAPT genes revealed similar potency of ASO-001933 across the species (Figure S7).

ASO-001933 distributes throughout the brain causing widespread knockdown of tau transcript in non-human primates

Due to the promising *in vitro* and *in vivo* profile, ASO-001933 was evaluated in Cyno monkeys using catheterized IT delivery as the route of administration. Distribution of the ASO and reduction of tau transcript were evaluated in various brain regions following different dose levels ranging from 4 to 16 mg and following either a single IT injection or two IT injections given 1 week apart. Brain tissue was harvested 2 weeks post last dose. Broad distribution of ASO-001933 was detected by *in situ* hybridization histochemistry (ISH) using a fluorescently labeled sense probe to ASO-001933, with the highest signal in cortical regions (Figures 5A–5D). Dose-dependent reductions in tau mRNA were detected by qPCR in a variety of brain regions, including the frontal cortex, hippocampus, and brainstem (Figure 6). All doses tested, 4–16 mg, provided greater than 50% tau mRNA lowering, and a single dose of 8 mg was sufficient to lower transcript by 80% 2 weeks after the injection. A loading dose paradigm, two injections of 8 mg 1 week apart, provided a modest improvement in tau knockdown in some brain regions examined over a single dose (Figure S11). Tau transcript knockdown in the sub-regions of the midbrain and brainstem, including the substantia nigra and pontine nuclei, areas known to be affected by tau pathology in PSP, was observed using a ^{35}S-labeled cDNA probe against tau transcript (Figures 5E–5H) and by ViewRNA fluorescent ISH (S10).

A

B

C

Figure 2. LNA pattern modifications altered ASO potency and tolerability both *in vitro* and *in vivo*

(A) IC_{50} (protein) and tolerability of hTau mouse primary neuronal cultures upon ASO treatments. Corresponding LNA pattern modifications are displayed along the x axis (L, LNA; D, DNA). ASOs with good tolerability (tubulin >70% UTC and CaOsc > 75%UTC), activity, and selectivity were selected for *in vivo* study. (B) Dose-dependent reduction of MAPT expression at protein level upon ASO-001933 treatment. hTau mouse primary neurons were treated with ASO-001933 at indicated concentrations. Tau protein levels were measured by high-content imaging (n = 15). (C) Assessment of *in vivo* acute tolerability and relative MAPT expression for each selected ASO. Each spot represents an ASO. ASO-001933 is shown in red.

LNA-modified ASOs are known to have higher affinity for their target compared with earlier generations of chemically modified ASOs.[33] Here we found that ASO-001933 given at a dose of 8 mg × 2 (16 mg total) produced up to 80% knockdown of both tau transcript and protein in cortex and hippocampus. Further exploration of the dose response revealed that a single injection of 8 mg produced comparable knockdown with the loading dose regimen in cortical regions, but with less effect in deep brain nuclei. Remarkably, even a single 4-mg dose was sufficient to achieve greater than 50% tau transcript lowering in the brain (Figure S11). These data indicate that the high affinity and *in vitro* po-

tency of LNA-modified ASOs confer higher *in vivo* potency of the molecule.

ASO-001933 has robust and sustained knockdown of tau protein in non-human primates

After establishing an optimal dose regimen of 8 mg given 2 weeks apart, a more detailed evaluation of the efficacy over time for mRNA and protein knockdown was then conducted using n = 3 control and n = 1 or 2 ASO-treated Cynos (Figures 6A–6C). ASO-001933 robustly lowered tau mRNA by 3 weeks post first dose in both frontal cortex and in the hippocampus (Figures 6A and 6B). Similarly, tau

Figure 3. ASO-001933 is a highly potent and selective ASO targeting MAPT on human neurons

(A) Schematic diagram of ASO treatment schedule in hESCs for (B)–(F). (B) Dose-dependent reduction of MAPT expression at RNA and protein level upon ASO-001933 or BIIB080 treatment. hESC-derived neurons were treated with ASO at indicated concentrations. RNA and protein levels were assessed by qRT-PCR and AlphaLISA respectively. Absolute IC_{50} values are reported in the figure (n = 3 /treatment, mean +/- SEM). (C) Quantification of 3R and 4R Tau mRNA by qPCR after ASO treatment at 1 μM (n = 3

(legend continued on next page)
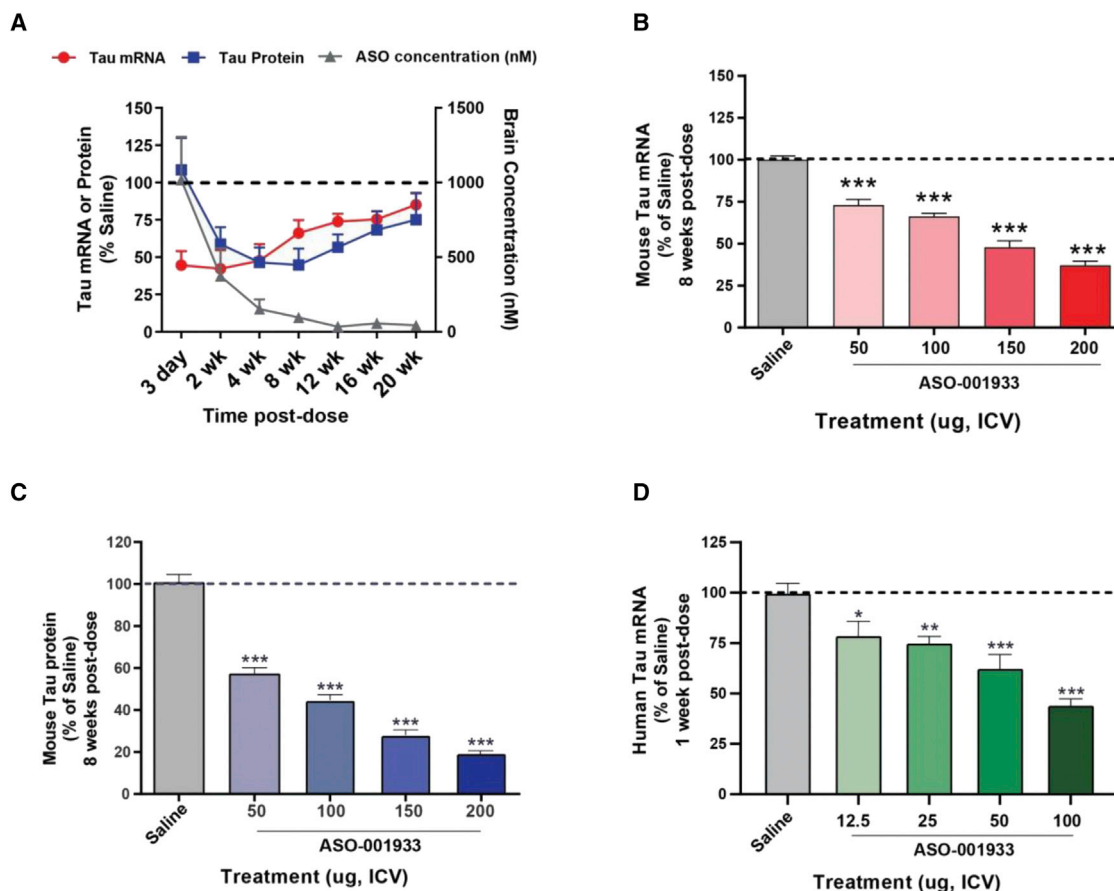
Figure 4. Single dose of ASO-001933 shows a robust and sustained reduction of mouse and human Tau *in vivo*

(A) ASO-001933 (100 μg ICV) time course for mouse tau mRNA (red circles) and tau protein (blue squares) in C57Bl/6J mice. ASO-001933 concentrations (gray triangles) in brain over the time course. (B) mTau mRNA is decreased by 70% 8 weeks after a single injection of 200 μg (n = 10–20/group, mean ± SEM). (C) ASO-001933 reduces mTau protein by 80% 8 weeks after a single injection (n = 9–19, mean ± SEM). (D) ASO-001933 reduces hTau mRNA by 1 week post injection (n = 10/group, mean ± SEM). Statistical analysis: one-way ANOVA with Dunnett's post hoc, *$p < 0.05$, **$p < 0.01$, ***$p < 0.0001$.

protein levels were also reduced up to 80% in frontal cortex and less in other brain regions (Figures 6A–6D). Highest efficacy was observed in cortical regions and in the hippocampus, with 70% tau protein lowering. Approximately 50% tau protein reduction was observed in ventral pons and medulla, whereas ventral midbrain shows the lowest efficacy with only 35% knockdown (Figure 6D). This outcome is likely due to differing exposure levels reached across these brain regions. The calculated *in vivo* IC$_{50}$ value of ASO-001933 was ∼500 nM in the brain and was found to be similar across brain regions.

Tau mRNA reduction was sustained out to 10 weeks post first dose, where an initial return to baseline levels could be detected. Tau protein was evaluated 3,6,10, 14, 18, and 22 weeks post first dose in various brain regions. As observed in the mouse time-course study, tau protein reduction lagged behind mRNA reduction, with maximal knockdown achieved 10 weeks post dose. Some variability in the time-course data was seen in the 14-week group, where we noted a slight increase in tau protein and mRNA that corresponded with somewhat lower brain concentrations in this cohort of animals. Strikingly, tau protein knockdown was sustained in both frontal cortex and the hippocampus out to 22 weeks post first dose, the final time point in the study (Figures 6A–6C). A mathematical model derived from the experimental data predicted a return to baseline by 50–60 weeks post dose, depending on the brain region. Tau protein analysis in the CSF reached maximal

/treatment, mean +/- SEM). (D and E) Representative images of RNAscope ISH and ICC using probes against MAPT CDS, MAPT 3′ UTR (D) and antibody against Tau (Tau HT7) (E). (F) Volcano plot illustrating differentially regulated proteins from proteomics analysis between ASO-001933-treated cells versus NT ASO-treated neurons (n = 3). MAPT is the only significantly regulated protein (Log2 FC = −2.94, adjusted Log10 p value = −4.54). (G) Evaluation of off-target effects of ASO-001933 in hiPSC-derived neurons. Volcano plot showing differentially expressed genes (Log2FC > 1 or Log2FC< −1 and −Log10 adjusted p >20) from RNA-seq analysis after 72 h of treatment (n = 3).
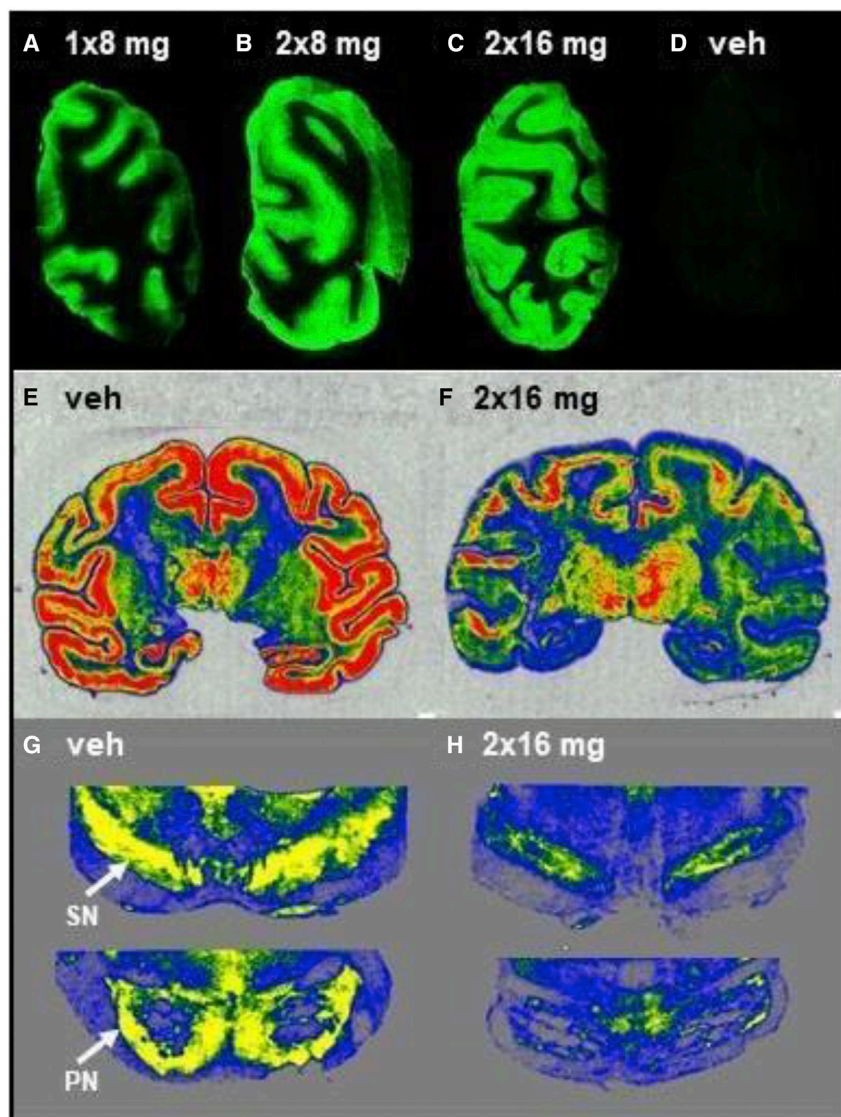
Figure 5. Broad ASO-001933 brain uptake and tau transcript lowering in NHP brains after IT delivery

ASO-001933 uptake in the frontal cortex of NHPs dosed with ASO-001933 at 1×8 mg (A), 2×8 mg (B), 2×16 mg (C), and vehicle (D), respectively. ASO-001933 is visualized with a fluorescently labeled sense probe. Pseudocolor green indicates ASO-001933 uptake. (E and F) Tau mRNA expression in the forebrain coronal section from the NHP dosed with vehicle or ASO-001933 at 2×16 mg. Tau mRNA expression is visualized with a ^{35}S-labeled antisense probe to Tau mRNA. Pseudocolor yellow/red indicates tau transcript expression. (G and H) Tau mRNA expression in the ventral region of the midbrain (upper) and pons (lower) of the NHP dosed with vehicle or ASO-001933 at 2×16 mg. Tau mRNA is visualized with a ^{35}S-labeled antisense probe to Tau mRNA. Pseudocolor yellow indicates tau transcript expression. SN, substantia nigra; PN, pontine nuclei. n = 1 or 2 monkeys/treatment group.

mated around 6–7 weeks but varied across brain regions following the variation in ASO uptake (Figure S12). Although the tau mRNA half-life could not be estimated in a straightforward manner due to the two consecutive doses and the lack of observation shortly after injection, a turn-over model was used to describe the protein knockdown, which had an estimated half-life of 24 days, very close to the reported value of 23 days[32] (Figure S12). With an 8-mg dose level, the steady state is achieved with an interval of dosing every 20 weeks (Figure 7B). This very long interval between dosing can be attributed to both the long ASO- and tau protein half-lives. Indeed, the half-life of ASO-001933 itself is approximately 6–7 weeks, a key factor determining the duration of knockdown. The long-lasting effects are comparable with, if not improved over, other CNS-targeting ASOs.[22,24,25] We speculate that, in addition to the phosphorothioate backbone, the LNA modifications may also contribute to good metabolic stability of ASO-001933.

lowering at 14 weeks post dose to 50% lagging behind brain protein reduction. Remarkably, a non-terminal study with CSF sampling from control (n = 2) and ASO-treated Cynos (n = 6) revealed a sustained tau protein lowering to final time point of 38 weeks post first dose with no clear sign of return to baseline, suggesting long-lasting effects of the ASO on CSF tau (Figure 6C). ASO-001933 was well tolerated in all studies; body weights were stable in monkeys treated up to 24 mg ASO and monitored for 6 weeks (Figure S8B).

A PK/PD model was derived from the pharmacokinetics of the ASO concentrations and the time course for tau mRNA and protein knockdown. We find that our non-human primate (NHP) PK/PD model recapitulates the difference in brain ASO-001933 uptake and clearance across brain regions and explains these differences in maximal knockdown and duration of action. The half-life of ASO-001933 was esti-

DISCUSSION

Here we report that we have identified an LNA ASO directed against the tau transcript with excellent drug-like properties, including high potency, selectivity, tolerability, and PK properties. ASO-001933 had single-digit nanomolar potency in mouse primary cultures, Cyno monkey neurons, and human neurons. RNA-seq and proteomics analyses of ASO-001933 treatment on human neurons demonstrated clear selectivity for tau over other targets. ASO-001933, administered directly into the ventricles of mice, robustly reduced endogenous mouse tau and human tau transcripts and protein. Following intrathecal delivery, the anticipated route of administration for ASOs in patients, robust knockdown of tau transcript and protein
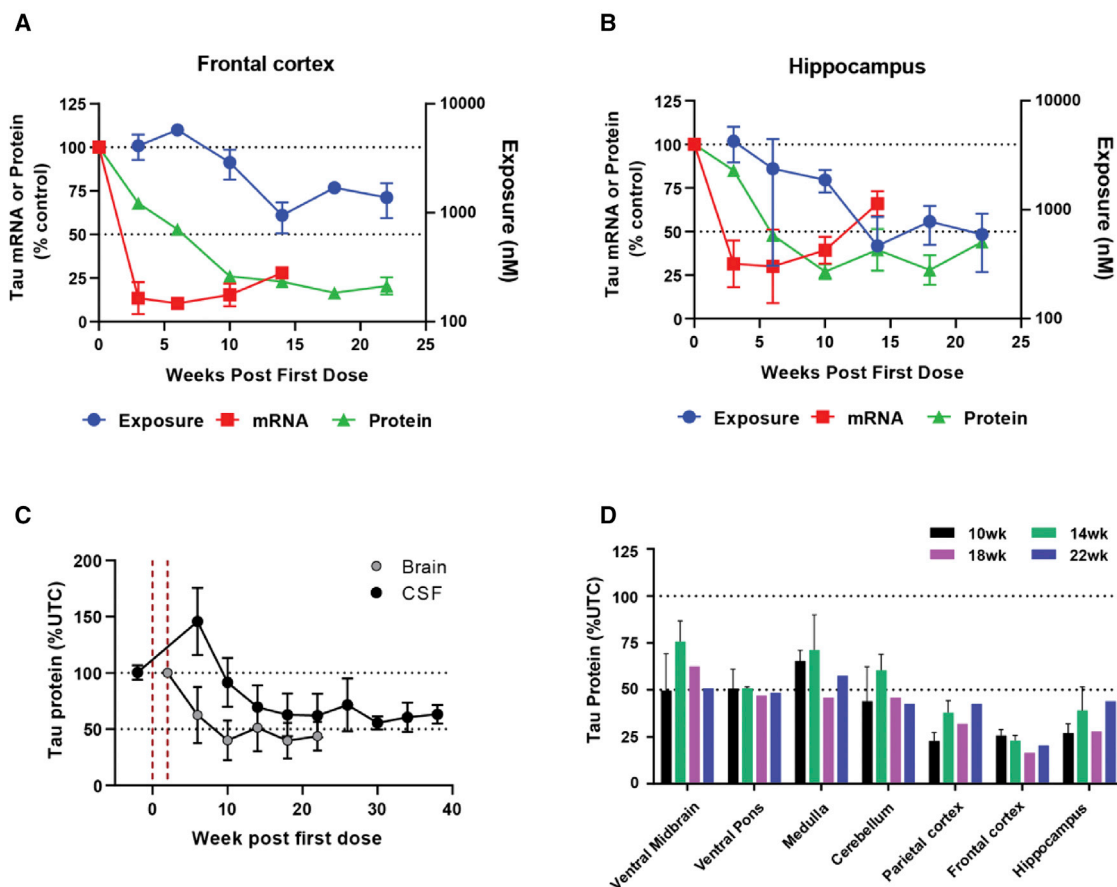
Figure 6. ASO-001933 has a long duration of action on tau in both brain and CSF in NHP brains after IT delivery

ASO-001933 (2 × 8 mg) produces robust mRNA and protein reduction in frontal cortex (A) and hippocampus (B). Brain tau protein lowering (average of the following brain regions: ventral midbrain, ventral pons, medulla, cerebellum, parietal cortex, frontal cortex, and hippocampus) predicted CSF tau protein lowering (C). Vertical dashed red lines indicate time of first and second 8-mg dose, respectively. Tau lowering was detected in all brain regions assessed with highest knockdown in frontal cortex and less in ventral midbrain (D). For CSF tau, n = 2 control and n = 6 ASO-treated monkeys. For brain tau, n = 3 vehicle-treated and n = 1 ASO-treated monkey at 6, 18, and 22 weeks post first dose, n = 2 ASO treated at 10 and 14 weeks post dose. UTC, untreated control. Data are represented as the group mean ± SEM.

was achieved throughout the brain in NHPs. Furthermore, ASO-001933 treatment showed a long duration of action in both mice and monkeys. Modeling of the NHP data indicated that an 8-mg dose given IT once every 20 weeks would be sufficient to maintain greater than 50% tau protein lowering in cortex and hippocampus. Taken together, our data indicate that molecules like ASO-001933 can have excellent drug-like properties and sustained efficacy predicting infrequent, intrathecal dosing in patients.

A key question for tau ASO therapeutics is to what extent tau transcript must be reduced to be protective. A large body of data demonstrates beneficial effects of tau lowering in preclinical models. Using a doxycycline-regulatable transgenic model, tau transgene expression lowering by 60%–85% resulted in reduced tau pathology, functional improvement, and neuroprotection in mice carrying a human, mutant Tau transgene.[34,35] Similarly, reduction of tau protein by approximately 50% with a tau ASO was shown to have benefit on tau pathology and

neurodegeneration in mouse.[22] Interestingly, even in disease models where mutant tau is not the pathogenic driver, tau deletion has been shown to have a benefit. In APP transgenic mice, mice heterozygous and homozygous for Tau deletion showed reduced synaptic, network, and behavioral dysfunction.[36-38] Similarly, deletion of one copy of tau was sufficient to reduce seizure activity and mortality in Scn1a^{RX/+} mice, a model of infantile epilepsy.[39] We previously reported preventative treatment with ASO-001933 significantly reduced mortality and epileptiform spike activity in Scn1a^{RX/+} mice, an effect associated with approximately 50% tau protein reduction.[40,41] Taken together, these data indicate that even 50% lowering of tau in disease-relevant brain areas may be sufficient for therapeutic benefit in CNS disease. Furthermore, ASO-001933 treatment would be anticipated to have benefit in all tauopathies given that 3R and 4R tau transcripts are reduced similarly.

Similar to other oligonucleotides tested in the NHP,[24,42] ASO-001933 did not distribute to all tissues equally. We found ASO concentration
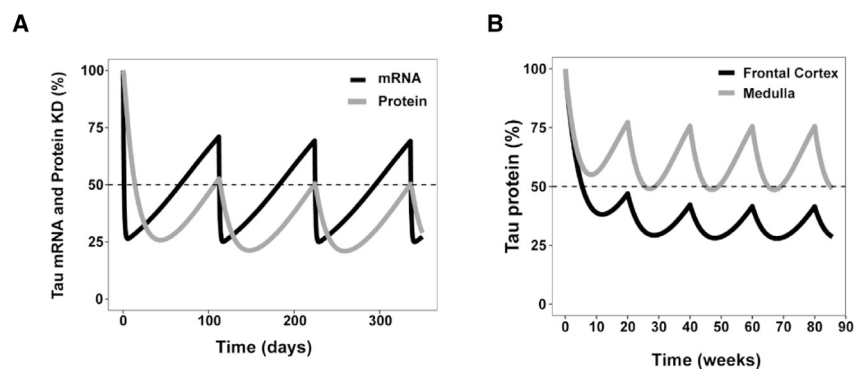
A

B

and knockdown highest in cortical regions and hippocampus with less knockdown in cerebellar nuclei, ventral midbrain, pons, and medulla. Similarly, IT delivery of a 2′-MOE gapmer against Malat1 produced broad knockdown across many CNS tissues with greatest knockdown in spinal cord followed by hippocampus and cortical regions, with less knockdown and more variability in caudate, putamen, thalamus, and deep cerebellar nuclei.[42] Because ASOs with different chemistries have similar distribution patterns following IT delivery, the distribution of ASOs may ultimately be limited by accessibility to brain regions distal to the ventricles and CSF compartment. However, our modeling data suggest that high, tolerated doses of ASO-001933 can achieve disease-relevant knockdown in deeper brain regions. To further improve tau knockdown in brain regions more difficult to target, methods to enhance ASO delivery[43] may be employed in future drug development programs. For example, ASOs can be conjugated to antibodies or sugars (e.g., GalNacs) or delivered in lipids to enhance delivery to specific tissues. So far, Alnylam has demonstrated success with GalNac-conjugated siRNAs.

Here we explored whether CSF tau can be used as a biomarker to determine the extent of tau lowering in the brain in patients. We were able to detect approximately 50% tau lowering in the CSF of monkeys, which was associated with 50%–80% tau protein lowering in the brain, depending on the region. Similarly, DeVos et al. reported a 25% decrease in CSF tau concomitant with 50% tau protein lowering in the brain.[22] It is encouraging to see similar datasets across laboratories, despite the technically challenging nature of measuring CSF tau following the surgical implantation of a catheter, which can acutely elevate injury-related markers.[44] In patients, CSF tau measures have been established and are routinely used as disease biomarker selection criteria or outcome measures in clinical trials.

Although significant characterization of ASO-001933 has been conducted, there are a few notable limitations to our work. First, a complete safety assessment was not conducted. Upon systemic dosing, class-related adverse effects have been reported due to accumulation of ASO in the kidney tubule.[45] Due to tau expression in glomeruli and regulation of kidney metabolism,[51] further evaluation of accumulation of ASO-001933 in kidney may be warranted; however, the risk of peripheral side effects is expected to be low when ASO is delivered

directly and infrequently into the CNS. Accumulation at the site of administration in the spinal cord may also require further evaluation in nonclinical species. Characterization of Tau KO mice has revealed metabolic, cognitive, and motor dysfunction in mice homozygous for the MAPT gene deletion, depending on the age and strain of the mice.[46-52] Few, if any, studies report adverse phenotypes in mice heterozygous for the MAPT deletion, indicating that 50% loss of wild-type transcript is anticipated to be safe in humans. One caveat to interpreting such studies is the use of a constitutive deletion of MAPT from birth, which differs from the intended therapeutic approach. To date, no behavioral or pathological side effects have been reported in nonclinical species with tau-lowering ASOs,[21-22] and safety data from on-going clinical studies with BIIB080 is forthcoming. A second limitation of the work presented here was that efficacy of ASO-001933 was not assessed in a Tau pathology model, although benefit on Tau pathology and neurodegeneration has been reported previously in Tau ASO-treated mice.[22] Additional data would increase confidence that reducing pathological forms of Tau, while simultaneously lowering wild-type tau, will provide benefit to patients.

Although the relationship between tau pathology and neurodegeneration has long been recognized, the industry is still in the midst of testing the first wave of tau-targeting therapeutics in patients. Determining the best therapeutic approach to reducing tau pathology is not simple as the most pathogenic forms of abnormal tau have not yet been conclusively identified and may differ across tauopathies[53-55] and among individual patients with AD.[56] An ASO therapeutic approach, however, is agnostic to the form of aggregated tau and can reduce both intracellular and extracellular tau. While further toxicology and efficacy evaluation of ASO-001933 or similar molecules will be important, this modality should provide an optimal strategy to test the tau hypothesis in tauopathy patients.

MATERIALS AND METHODS
Oligonucleotide synthesis and purification
Single-stranded DNA oligonucleotides with complete phosphorothioate backbones and LNA-modified flanks were synthesized on a MerMade 192× synthesizer, MerMade 12 synthesizer (LGC Bioautomation, MI, USA) or an Äkta OligoPilot 100 synthesizer (Cytiva Life Science) utilizing standard phosphoramidite chemistry. For synthesis in small scale, the final 5′-dimethoxytrityl (DMT) group was left on the oligonucleotide for later use as a lipophilic handle during chromatographic purification and for synthesis in larger synthesis scale, the DMT group was removed from the oligonucleotide prior to cleavage and deprotection.

The oligonucleotides synthesized in small scale were cleaved from the solid support on a Hamilton Starlet pipetting robot (Hamilton, Bonaduz, Switzerland) using concentrated aqueous ammonia followed by deprotection in an oven at 65°C for 5–12 h. The oligonucleotides containing 5′-DMT were purified by solid phase extraction in TOP cartridges (Agilent Technologies, Glostrup, Denmark) supported on a Hamilton Starlet pipetting robot (Hamilton, Bonaduz, Switzerland). The full-length oligonucleotide having a 5′-DMT group binds to the column material of the cartridge, allowing for removal of shorter failure sequences. Subsequent removal of the DMT group allowed for elution of the purified oligonucleotide. The collected solution of purified oligonucleotide was evaporated to dryness and subsequently dissolved in PBS. The concentration of oligonucleotide in solution was determined by calculating the Beer-Lambert extinction coefficient and measuring the UV absorbance of the solution at 260 nm. Oligonucleotide identity and purity were validated by reversed-phase ultra-performance liquid chromatography coupled to MS (UPLC-MS).

Cleavage and deprotection of oligonucleotides synthesized in larger synthesis scale (e.g., 20–500 μmol) was performed using a concentrated solution of aqueous ammonia overnight at 65°C. The solid support was removed by filtration and the solution lyophilized overnight. Subsequent purification by ion-exchange high-pressure liquid chromatography (HPLC) chromatography at elevated pH using a gradient of NaCl afforded the purified oligonucleotide. The solution was neutralized and desalted by either size-exclusion chromatography (Äkta Pyrified, Cytiva Life Science) or tangential flow filtration (Äkta CrossFlow, Cytiva Life Science) and the oligonucleotide could be collected after lyophilization. Oligonucleotide identity and purity were validated by reversed-phase UPLC-MS followed by a test for the presence of endotoxins (Endosafe, Charles River Labs). Oligonucleotides with an endotoxin content below 0.2 EU/mg were released for use.

In vitro methods
Mouse primary neuronal culture
Each of the oligomers targeting the 3′ UTR of an *MAPT* transcript was tested for its ability to decrease tau protein in mouse primary neurons expressing the entire human *MAPT* gene as a bacmid containing transgene.[22] Primary hTau mouse embryonic forebrain neuronal cultures do not express endogenous mouse tau as mouse tau was knocked out. Primary neurons were generated by papain digestion according to manufacturer's protocol (Worthington Biochemical Corporation, LK0031050). Briefly, forebrains were dissected from hTau mouse El 8 BAC-Tg embryos expressing the entire human microtubule-associated protein tau (*MAPT*) gene on a murine MAPT-nuW background and were incubated at 37°C for 30–45 min in papain/DNase/Earle's balanced salt solution (EBSS). After trituration and centrifugation of cell pellet, the reaction was stopped by incubation with EBSS containing protease inhibitors, bovine serum albumin (BSA), and DNase. The cells were triturated and washed with Neurobasal (NB, Invitrogen) supplemented with 2% B-27, 100 μg/mL penicillin, 85 μg/mL streptomycin, and 0.5 mM glutamine. The cells were plated in supplemented NB media onto poly-D-lysine-coated 96-well optical imaging plates (BD Biosciences) at 15,000 cells/well.

After obtaining the primary hTau mouse embryonic forebrain neuronal cultures expressing a human *MAPT* gene, the cultures were treated with oligomers to inhibit the tau mRNA and protein expression. The cultures were then subject to immunocytochemistry and imaging to measure the inhibition. One day post plating (DIV 1), half of the supplemented neurobasal (NB) media on the primary hTau mouse embryonic forebrain neuronal cultures was removed and replaced with supplemented NB medium containing various concentrations of LNA oligomers. Primary hTau neuronal cultures were cultured with LNA oligomers until 13 days post plating (DIV 13). On DIV 13, the cultures were rinsed with Dulbecco's phosphate-buffered saline lacking calcium and magnesium (DPBS, Invitrogen) and fixed in 4% paraformaldehyde/4% sucrose/DPBS for 15 min. Cultures were rinsed and then blocked and permeabilized in DPBS plus 0.1% Triton X-100 (TX-100) and 3% BSA for 1 h at room temperature. Cultures were rinsed and then incubated for 2 h at room temperature with primary antibody (1:500 Tau5 antibody to measure tau protein [Invitrogen AHB0042] and 1:500 β-III tubulin [TuJ-1] antibody to measure neurite area; Abeam ab41489) in DPBS plus 3% BSA and 0.1% TX-100. Cultures were rinsed and incubated with Hoechst 33342 nuclear dye (1:800, Invitrogen) and AlexaFluor fluorescence-conjugated secondary antibodies (Invitrogen, 1:500) in DPBS plus 3% BSA and 0.1% TX-100 for 1 h at room temperature. Cultures were rinsed abundantly and stored in DPBS until imaging. Imaging was conducted using the Cellomics VTi automated immunofluorescence imaging system. In brief, using untreated wells, saturation levels for each fluorophore channel were set to 70%. Then 12 sequential images were acquired from each well, and total fluorescence intensity and total fluorescence area were calculated for both Tau and tubulin proteins using the Cellomics VTi SpotDetector (version 4) image analysis software. To evaluate Tau protein reduction resulting from oligomer treatment, a Tau5 total fluorescence intensity-to-Tuj-1 total fluorescence area ratio (Tau/TuJ-1) was created for each well and then all data were normalized to the average Tau/Tuj-1 ratio of the untreated wells. TuJ-1 intensity acts as an internal standard for each sample. To evaluate neurite/neuronal toxicity from oligomer treatment, the Tuj-1 total fluorescence area from each well was normalized to the average Tuj-1 total fluorescence area of the untreated wells. Nuclei counts from each well were also acquired as an alternative measure of toxicity associated with LNA oligomer treatment. Data are expressed as mean ± SD. For immunocytochemistry, data points represent the mean ± SD from wells treated in triplicate. Potency values were generated using wells treated with a broad concentration range of LNA oligomer, from which the resulting normalized Tau/Tuj-1 and Tuj-1 values were analyzed compared with normalized values from saline control samples. Analysis was done using non-linear regression with top and bottom values set at fixed values of 100% and 0%, respectively, where 100% inhibition represents a complete reduction of signal compared with the control sample (Figure 2). For qPCR, data were analyzed using a one-way ANOVA with a Dunnett's multiple comparison test to compare saline- and LNA oligomer-treated groups. Statistical significance was set at a value of $p < 0.05$.

Calcium oscillation assay

Primary cortical neurons were prepared from Sprague-Dawley rat embryos on embryonic day 19. Cells were plated with 25,000 cells/well onto 384-well poly-D-lysine-coated fluorescent imaging plate reader (FLIPR) plates (Greiner Bio-One) in 25 µL/well neurobasal media containing B27 supplement and 2 mM glutamine. Cells were grown for 11 days at 37°C in 5% CO_2 and fed with 25 µL of additional medium on days 4 and 8. On the day of the experiment, medium was removed from the plate and the cells were washed once with 50 µL/well of 37°C assay buffer (Hank's balanced salt solution with 2 mM $CaCl_2$ and 10 mM HEPES [4-(2-hydroxyethyl)-1-piperazineethanesulfonic acid] pH 7.4). Calcium oscillations were measured in the presence and absence of 1 mM $MgCl_2$.

Cells were loaded with a cell-permeant fluorescent calcium indicator dye, fluo-4 AM (Life Technologies). Fluo-4 AM was prepared at 2.5 mm in dimethyl sulfoxide containing 20% plutonic F-127 and then diluted 1:1,000 in assay buffer. Cells were incubated for 1 h with 20 µL of 2.5 mM fluo-4 AM at 37°C in 5% CO_2. After 1 h, 20 µL of room temperature assay buffer was added and the cells were allowed to equilibrate to room temperature for 10 additional minutes and placed in the FLIPR.

For studies used to identify ASOs for advancement to evaluation in mice, a method of quantification was designed to capture both increases and decreases in oscillation frequency following ASO treatment. First, baseline signal of intracellular calcium levels was read for 100 s (one reading per second) before the addition of ASO. ASOs were added with a 384-well head in the FLIPR in 20 µL of assay buffer at 75 µM for a final concentration of 25 µM. FLIPR signal was read for an additional 200 s (one reading per second) after the addition of ASO. After 5 min, a second read of FLIPR signal was conducted for 300 s (one reading per second) to allow for additional data capture.

Spike amplitude and frequency of calcium oscillations were calculated from FLIPR signal reads. An average control value was established by measuring the average FLIPR spike amplitude signal over a 300-s read for nontreated wells. A scoring system was developed where a score of 1 was given for each 1-s read where signal increase was >50% of the average control amplitude value. A score of 0 was given for each 1-s read, which increased <50% of average control amplitude value. For each ASO, the total summed score was calculated and converted to percentage of control.

Neuronal cell culture medium

N2B27 medium is composed of DMEM/F12 supplemented with modified N2 supplement and Neurobasal medium supplemented with B27 supplement minus vitamin A, in a 1:1 ratio and 50 µM β-mercaptoethanol (Thermo Scientific). FEB medium is N2B27 medium supplemented with 10 ng/mL FGF-2 (Peprotech), 10 ng/mL EGF (R&D Technologies), and 20 ng/mL BDNF (Peprotech). SFA medium is N2B27 medium supplemented with 100 ng/mL FGF-8 (Peprotech), 200 ng/mL sonic hedgehog (Peprotech), and 100 µM ascorbic acid 2-phosphate (Sigma). BGAA medium is N2B27 medium supplemented with 20 ng/mL BDNF, 10 ng/mL GDNF (Peprotech), 500 µM dibutyryl cyclic AMP (Sigma), 100 µM ascorbic acid 2-phosphate, 100 units/mL of penicillin, 100 µg/mL of streptomycin (Pen-Strep, Thermo Scientific), and 2 µg/mL Laminin (Roche).

Cyno NPC differentiation medium is composed of Neurobasal medium supplemented with B27 supplement (Thermo Scientific) and GlutaMAX supplement (Thermo Scientific), 20 ng/mL BDNF, 10 ng/mL GDNF, 100 µM ascorbic acid 2-phosphate, 100 units/mL of penicillin, 100 µg/mL of streptomycin, and 2 µg/mL Laminin.

Human neuronal cell culture and LNA treatment

The hESC line SA001 (NIH registration number 0085; Cellectis, Sweden) derived NPCs were dissociated with Trypsin-EDTA 0.05% (Thermo Scientific), plated on polyornithine-/laminin-coated (PL) flasks/dishes at 10,000 cells/cm^2 in SFA medium, and cultured for 1 week with medium replacement after 3–4 days. The resultant progenitors were dissociated with trypsin/EDTA 0.05%, plated on PL flasks/dishes at 50,000 cells/cm^2 in BGAA medium and differentiated for 6 weeks with medium replacement every 3–4 days. ASO-001933 or NT LNA was incubated at indicated concentration from day 0, unless otherwise noted, and LNA was maintained in the cell culture medium. Human iPSC (hiPSC)-derived glutamatergic neurons were used in evaluation of off-target effects (Figure 3G), which were purchased from FujiFilm Cellular Dynamics (catalog no. R1034). Plating and maintenance of the cells was performed according to the manufacturer's instructions.

qRT-PCR analysis of tau mRNA in human neurons

RNA for qPCR was extracted from cells using the Qiagen RNeasy Kit according to the manufacturer's protocol. Expression of target genes was quantified using qScript XLT 1-Step RT-qPCR mix (Quanta Bioscience) and TaqMan Gene Expression Assays (Thermo Scientific). qRT-PCR was done on Applied Biosystem ViiA 7 Real-Time PCR System. The following TaqMan gene expression assays were used: MAPT (Hs00902193_m1) and TBP (#4326322E; reference gene). Relative expression levels of tau were calculated using the delta-delta Ct method.

qRT-PCR of 3R and 4R tau isoforms in human neurons

For quantification of 3R and 4R tau RNA levels after ASO-001933 treatment, expression of target genes was quantified using Power SYBR Green RNA-to-CT 1-Step Kit (Thermo Scientific). qRT-PCR was done on Applied Biosystems Quantstudio 12 k flex Real-Time PCR System. The following primers were used: 3Rtau F AGGC GGGAAGGTGCAAATAG, 3R tau R TCCTGGTTTATGATGGA TGTT, 4R tau F GAAGCTGGATCTTAGCAACG, 4R tau R GACG TGTTTGATATTATCCT, GAPDH F GGAGCGAGATCCCTCCA AAAT and GAPDH R GGCTGTTGTCATACTTCTCATGG (reference gene).

Bulk RNA-seq and differential expression analysis

RNA isolation was performed using RNeasy Mini Kit (Qiagen) following the manufacturer's instructions. Total RNA-seq libraries

were constructed and further sequenced at Fasteris (Switzerland). Sequencing libraries were generated using TruSeq stranded total RNA library preparation protocol with RiboZero to remove rRNA (Illumina). Libraries were subjected to paired end sequencing on a NovaSeq6000 sequencer (Illumina) with 150-bp read length. Sequencing depth was ~35 Mio. The reads of the samples were aligned to the human reference genome (GRCh38) using STAR and sorted using SAMtools. The quantification and annotation were performed using RSEM. The differential expression analysis on the samples was performed using DESeq2 in R.[57] Raw data are deposited in NCBI Gene Expression Omnibus (GEO) repository under GEO accession GSE204930.

Tau and pTau protein measurement (AlphaLISA)

Cells cultured in 96-well plates were lysed in CytoBuster Protein Extraction Reagent (Millipore) supplemented with Phosphostop (Roche), cOmplete EDTA-free Protease Inhibitor (Roche), DNase I recombinant (Roche), and 10 mM $MgCl_2$ for 5 min at room temperature. Tau levels in extracts were measured by AlphaLISA using a Roche proprietary assay format comprising tau-specific antibodies 5A6 and tau-4/2 (generated internally at Roche). A standard curve prepared using recombinant human tau is used to determine the tau level. Tau-pS422 levels in extracts were measured by AlphaLISA using a Roche proprietary assay format comprising tau-specific antibody 5A6 and tau-pS422-specific antibody 5.6.11 (generated internally at Roche). A standard curve was prepared using ERK-phosphorylated tau where the extent of phosphorylation at the S422 epitope had previously been determined by MS. Cell extracts were diluted 20-fold into AlphaLISA HiBlock buffer (PerkinElmer) for assay. In a 384-well plate, 5 μL of standard or sample, 10 μL of 5A6-biotinylated antibody at 10 nM, and 10 μL of tau 4/2 or tau 5.6.11 coupled AlphaLISA Acceptor Beads (1/100) were mixed and incubated for 1 h at RT with shaking. For the detection, 25 μL of streptavidin donor beads at 80 μg/mL were added and incubated for 30 min with shaking and then read on EnVision (with Alpha module). The concentration of tau or tau-pS422 calculated for each cell extract was normalized to the total protein concentration in the cell extract as measured by BCA assay.

ICC

Cells cultured in 96-well plates (BD Falcon) were fixed in 4% paraformaldehyde (PFA) in PBS for 10 min, permeabilized with 0.2% (v/v) Triton X-100 in PBS for 10 min, and incubated for 30 min in blocking solution (3% BSA in PBS w/v). Primary antibodies were diluted in 3% BSA in PBS (w/v) and incubated for 1 h at room temperature. Wells were washed three times with PBS Tween 0.1% (Thermo Scientific). Secondary antibodies were diluted in PBS Tween 0.1% and incubated for 1 h at room temperature. Cells were incubated with PureBlu DAPI (Bio-Rad) in PBS for 3 min at room temperature. Wells were washed with PBS and stored at 4°C. Confocal images were obtained on Leica SP5 and imaging settings were kept constant for all treatment groups. Primary and secondary antibodies and dilutions used here were as follows: TAU-5 (Thermo Scientific; AHB0042, 1:200), MAP2 (Thermo Scientific; PA1-10005, 1:3,000), goat anti-mouse Alexa Fluor 488 (Thermo Scientific; A-11001, 1:500), goat anti-chicken Alexa Fluor 647 (Thermo Scientific; A-21449, 1:500).

RNAscope FISH

FISH on cells cultured in 96-well plates was performed according to the manual for cultured cells using the RNAscope fluorescent multiplex assay (Advanced Cell Diagnostics). After FISH, cells were counterstained with PureBlu DAPI (Bio-Rad) in PBS for 3 min at room temperature. Wells were washed with PBS and stored at 4°C. Confocal images were obtained on a Leica SP5. The following probes were used for detection of MAPT CDS and MAPT 3′ UTR: RNAscope Probe Hs-MAPT-C3 (Advanced Cell Diagnostics; 408991-C3) and RNAscope Probe Hs-MAPT-O1 (Advanced Cell Diagnostics; catalog no. 485981).

Protein profiling by MS

Neurons were harvested at day 42 post differentiation and were resuspended in lysis buffer (iST buffer Preomics, Martinsreid) with protease inhibitor cocktail (Roche). Samples were boiled at 95°C for 10 min and sonicated in a bath sonicator (Bioruptor Plus, Diagenode) for 10 cycles (15 s on, 15 s off). Post lysis, protein estimation was performed using the BCA assay (Sigma-Aldrich) and 50 μg of total protein was digested into peptides using the Preomics kit (Preomics, Martinsreid). Peptides corresponding to 1 μg of protein were measured on the Orbitrap Fusion instrument (Thermo) in data-dependent acquisition (DDA) mode. Peptides were analyzed by nano-liquid chromatography-tandem mass spectrometry (LC-MS/MS) (Easy LC 1200, Thermo Scientific) coupled to the Orbitrap Fusion mass spectrometer (Thermo). Peptides were trapped on a 5-mm Pepmap 100 C18 column (300-μm internal diameter [i.d.], 5-μm particle size, from Dionex) and fractionated on a 500-mm Alltima C18 column (100-μm i.d., 3-μm particle size). The acetonitrile concentration in the mobile phase was increased from 5% to 17% in 17 min, to 45% in 120 min, and to 100% in another 20 min, at a flow rate of 300 nL/min. The eluted peptides were electro-sprayed into the Orbitrap Fusion instrument run in DDA mode. The nano-spray needle voltage was set to 2,100 V. The mass spectrometer was operated in a data-dependent mode with a single MS full scan (m/z 300–1,500, maximum injection time = 100 ms, Orbitrap resolution = 120,000). Top MS1 (charges 2–6) peptides were isolated with a window of 1.8 m/z; activation type, HCD; collision energy was set to 30%, with an exclusion time of 75 s once the peptide was fragmented.

The MS raw data were imported into MaxQuant (v 1.6.5.0), and searched against the Swissprot human proteome (SwissProt, September 2020 release) with oxidation (M), acetyl (protein N-term), carbamidomethyl (C), and N-terminal acetylation as variable modifications. Unique peptides were used for quantification. For both peptide and protein identification, a false discovery rate of 0.01 was set, and MaxLFQ normalization was enabled with an LFQ minimal ratio count of 1; further MaxQuant settings were left at default. The MaxQuant search results are provided in Table S1. Protein groups file was imported into Perseus (v 1.6.14.0) and pairwise statistical analysis (false discovery rate [FDR] <0.05, S0 = 0.1) was

performed post data filtering (removal of contaminants, reverse entries, minimum three valid values per condition).

In vivo methods
Animals
Adult female C57Bl/6J mice (20–30 g; Jackson Laboratories, Bar Harbor, ME) housed three or four per cage were used to assess tau lowering following ASO delivery. In some experiments, male and female PAC transgenic mice (30–40 g) expressing a human genomic tau transgene driven by the tau promoter,[26,33] and in which the native mouse tau gene was deleted, were used to confirm ASO activity on the human tau transcript. Mice were held in colony rooms maintained at constant temperature ($21°C \pm 2°C$) and humidity ($50\% \pm 10\%$) and illuminated for 12 h per day (lights on at 0600 h). Food and water were given *ad libitum*.

Adult male Cyno monkeys weighing 3.5–10.0 kg at the start of each study were implanted using aseptic techniques with an intrathecal CSF catheter entering at the L3 or L4 vertebra extending to approximately the L1 vertebra. The proximal end of the catheter was connected to a subcutaneous access port. Animals were pair housed as appropriate. Access to food and water were not restricted.

Mouse intra-cerebroventricular injections
The oligomers were administered to C57Bl/6J or hTau mice by ICV injection in a concentration of 20–40 mg/mL in a volume of 5 mL in 0.9% saline. The counterions were equivalent between all compounds as all ASOs were sodium salts. The contribution of the ASO chain and the associated sodium ions to the formulation osmolarity were minor at dosing concentrations used. Intracerebroventricular injections were performed using a Hamilton microsyringe fitted with a 27- or 30-gauge needle, according to the method of Haley and McCormick.[58] The needle was equipped with a polyethylene guard at 2.5 mm from the tip in order to limit its penetration into the brain. Mice were anesthetized using isoflurane anesthetic (1.5%–4%). The needle tip was then inserted through the scalp and the skull into the right lateral ventricle, about 1 mm lateral and 0.5 mm caudal to bregma. The needle was left in place for 10 s before removal. This procedure required no surgery or incision. Animals were warmed on heating pads until they recovered from the procedure. For 1 h following the single bolus injection of ASO, animals were observed for acute behavioral side effects using a modified Irwin battery.[27,31] At pre-specified time points (days or weeks post injection), brain tissue was collected on dry ice or RNAlater for drug concentration analysis, tau qPCR, and protein measurement.

Mouse and NHP brain Tau mRNA analysis
For the dose-response and time-course studies, C57Bl/6J mice were treated with ASO, and bulk tissue from the right frontal cortex was collected for mRNA analysis. In monkey, areas of interest were dissected using 6-mm slices in an ASI Cyno Brain Matrix as well as freehand techniques. Samples were placed fresh in RNAlater for later analysis. In both cases, similar protocols were used. Total RNA was extracted using RNeasy Mini Kit (Qiagen) following manufacturer's

instructions. For cDNA synthesis and subsequent PCR, 300 ng of RNA from brain tissue was added to one well of a 96-well plate (Axygen, PCR-96-C-S). To each well, 7.5 μL of master mix (5 μL of 2.5 mM NTP mix and 2.5 μL of random primers per reaction) was added and the plate was centrifuged at 1,000 rpm and placed in thermocycler for 3 min at 70°C. Plates were immediately cooled on ice and 4 μL of reaction master mix was added. Prior to PCR, plates were briefly centrifuged to collect sample in the bottom of the well. cDNA synthesis was carried out at 42°C for 60 min, 95°C for 10 min, followed by a hold at 4°C. cDNA samples were diluted 1:3 with molecular-biology-grade water and stored at $-20°C$ until further use. For PCR, each sample was run in triplicate with two probe sets (MAPT, Taqman Expression assays Hs00902193_ml; GAPDH Taqman Expression assays Hs01922876_m1). To each reaction, 4 μL of previously diluted cDNA and 6 μL of master mix was added and plates were centrifuged. Samples were incubated at 95°C for 20 s follow by 40 cycles at 95°C for 1 s and 60°C for 20 s. Data were analyzed using the delta-delta Ct method, where each sample is first normalized to GAPDH and then expressed as percentage of untreated control animals.

Mouse Tau protein ELISA
Mouse brain tissue was homogenized in a $10\times$ volume of a high-salt/sucrose buffer (10 mM Tris-HCl, pH 7.4, 800 mM NaCl, 10% sucrose [w/v], 1 mM EGTA) supplemented with phosphatase inhibitor cocktail sets 2 and 3, 1 mM PMSF (Sigma, Saint Louis, MO), and complete protease inhibitor cocktail EDTA-free (Roche, Indianapolis, IN) using a Qiagen TissueLyzer II. The homogenate was centrifuged at $20,000 \times g$ for 20 min at 4°C. The supernatant was centrifuged at $100,000 \times g$ for 1 h at 4°C and the supernatant was analyzed.

The BT2 (antibody to tau amino acid 194-198, Thermo Scientific) was used to coat 96-well black ELISA plates (Costar) at a concentration of 2.5 g/mL for 1 h at 37°C. After washing in tris-buffered saline (TBS) containing 0.05% tween-20 (TBST), the plates were blocked with 3% BSA in TBS. Recombinant human tau441 (rPeptide; Bogart, GA) or a 1:5,000 dilution of the brain homogenates were diluted in 1% BSA + 0.05% Tween-20 in TBS. Alkaline phosphatase-conjugated Tau-5 (antibody to tau amino acid 210-230, Covance, Emeryville, CA) was added to the samples at a 1:2,000 dilution for co-incubation overnight at 4°C with shaking. After washing in TBST, the signal was amplified with the Tropix CDP-Star detection reagent from Applied Biosystems. The chemiluminescent signal was read on an Envision (Perkin Elmer). For CSF samples, this ELISA was done in a 384-well format to minimize the volume of CSF needed. Ten milliliters of a 1:2 dilution of CSF was added to each well.

NHP CSF dosing, collection, and analysis
Cynos were administered with ASO-001933 (n = 6), which was dissolved in saline, at 0.33 mL/min in a 1.0 mL volume followed by a 0.5 mL of sterile water flush. Total infusion time was 4.5 min. Control animals (n = 2) received 1.5 mL of saline at the same rate. Animals were dosed while conscious and in a horizontal position for at least 20 min after the infusion. At various time points, CSF was collected through the port by gravity flow to a maximum of 0.5 mL of CSF

per sample while the animals were awake and seated in a primate chair. The CSF was centrifuged and the supernatant was kept at −90°C until analyzed. Prior to necropsy, subjects were administered the appropriate volume of a commercially available euthanasia solution while anesthetized with ketamine. Necropsy tissues were obtained immediately thereafter and the brain was transferred to wet ice for dissection.

Tau ELISA for monkey samples

To measure tau protein expression in brain, an N-terminal assay was used. Specifically, Tau12 (BioLegend, San Diego, CA, epitope to amino acids 6–18 on tau 441 sequence) and BT2 (Thermo Scientific, Rockville, IL, epitope to amino acids 194–198) antibodies were used to coat Costar 3925 ELISA plates at 2.5 and 1 mg/mL, respectively. Plates were incubated for 1 h at 37°C before washing with TBST. Non-specific binding was blocked by the addition of 3% BSA in TBS with 0.1% Tween 20 for 4 h at room temperature with shaking. Plates were washed with TBST before the addition of samples or standard curve generated with recombinant h-tau441 protein, both of which were prepared in TBST plus 1% BSA. Plates containing standard curve and samples were incubated overnight at 4°C with shaking. The following detection antibodies were conjugated with alkaline phosphatase (AP) using the Lightning Link Conjugation Kit (Novus Biologicals, Littleton, CO): BT2 and HT7 (Thermo Scientific, epitope of 159–163). AP-conjugated detection antibodies were diluted in TBST plus 1% BSA and co-incubated with samples and standard curve for 1 h at room temperature with shaking. After washing with TBST, Tropix CDP-Star Ready-to-Use with Sapphire-II AP substrate (Applied Biosystems, Bedford, MA) was added for 30 min. Chemiluminescent signal was determined using a Perkin Elmer EnVision microplate reader (Waltham, MA).

To measure tau protein expression in CSF, the N-terminal tau sandwich ELISA (Tau12-BT2) consists of the anti-tau antibody Tau2 as capture and detection with an AP conjugate of the anti-tau antibody BT2. We have found that the N-terminal assay correlates very well (n = 121; R^2 = 0.74, p < 0.0001) with the mid-domain tau sandwich ELISA (BT2-HT7), so we chose to only run the N-terminal assay on the samples from this study. High-binding black-well ELISA plates (Costar, Corning, Tewksbury, MA) were coated with anti-Tau BT2 monoclonal antibody (Thermo, Waltham, MA) at 2.5 g/mL or Tau12 anti-tau monoclonal antibody (Covance) at 5 g/mL in TBS (50 II). The plates were washed with TBST followed by blocking at room temperature with shaking in 3% BSA/TBS (BSA from Roche, Indianapolis, IN). The plates were rewashed as listed above followed by sample addition in triplicate (50 m II). Cyno monkey CSF samples were diluted 1:30 (BT2/HT7) or 1:25 (Tau12/BT2) in 1% BSA/TBST. A Tau 441 (rPeptide, Bogart, GA) standard curve was made. The samples were incubated on the ELISA plate overnight at 4°C with shaking. AP-conjugated HT7 or BT2 was diluted to 0.25 mg/mL (HT7) or 0.1 mg/mL (BT2) in 1% BSA/TBST and was added to the plates for co-incubation with standards and samples for 1 h at room temperature with shaking. The plates were rewashed followed by the addition of chemiluminescent substrate (Tropix CDP-Star, Applied Bio-

systems, Grand Island, NY) and incubation at room temperature with shaking for 30 min. The plates were read on a Perkin Elmer TopCount. Unknown sample values were read off the Tau-441 standard curve using GraphPad Prism software.

ISH

Frozen monkey brain blocks were cut on a cryostat and coronal sections (50-μm thick) were thaw mounted onto super-frost slides for ISH studies. In order to visualize the brain tissue uptake and distribution of ASO-001933 following intrathecal administration, a sense probe against ASO-001933 was custom synthesized and labeled with a fluorescence marker (Affymetrix, Thermo-Fisher Scientific, Waltham, MA). Tau lowering was also visualized using an anti-sense QuantiGene probe to MAPT (region 2344-3300). The brain sections were processed with the probes following the QuantiGene ViewRNA tissue ISH procedure. In brief, after fixation in formaldehyde, sections were hybridized with the sense probe. Slides were then processed through a series of sequential PreAmplification and Amplification hybridization steps. The sections (n = 3–5/animal, one or two animals per treatment group) were then incubated with Label Probe AP and coverslipped. Slides were examined using a Leica confocal fluorescence microscope (excitation, 630 nm; emission, 760 nm).

In order to assess spatial tau mRNA knockdown, a tau DNA template and 35S-labeled antisense probes were synthesized. A tau DNA template (425 bp, 687–1,111, accession number: XM_005584540.1) was amplified from a Cyno monkey cDNA library (Zyagen KD-201) by PCR using forward primer 5′-CAAGCTCGCATGGTCAGTAA-3′ (sequence ID no. 954) and reverse primer 5′-AATTAACCCTCAC TAAAGGGAGATTCTCAGTGGAGCCGATCTT-3′ (sequence ID no. 955). Products of desired size were observed by gel electrophoresis. The tau DNA template was transcribed with T3 RNA polymerase (Invitrogen AMI 316) using 35SUTP (Perkin Elmer NEG-739) to produce a 35S-labeled antisense probe. After fixing in paraformaldehyde, sections were incubated in acetic anhydride/triethanolamine and prehybridized in the prehybridization solution, and brain sections from one animal per treatment group were hybridized with 1.5 × 10⁴ cpm/μL 35Sriboprobe (0.75 mL/slide) in hybridization solution. After hybridization, slides were washed and then treated with RNase A. The sections were then dried and exposed against phosphor screen (Perkin Elmer, Waltham, MA). After exposure, autoradiographic images on the screen were captured using Cyclone storage phosphor system and OptiQuant Acquisition and Analysis software (PerkinElmer, Waltham, MA). Tissue came from three to five sections per animal, and one or two brains per group were imaged. Images were used to provide a qualitative assessment of knockdown across the brain.

ASO-001933 PK analysis by ELISA

The ASO concentrations in tissue, plasma, and CSF from mouse or Cyno were determined by ELISA. The tissue samples were homogenized with the respective species plasma:water (1:1) diluent in a weight to volume ratio of 1:5. The CSF samples were 2-fold diluted with the respective species plasma. The samples were then further

2-fold diluted with Clarity OTX Lysis Buffer (Phenomenex, Torrance, CA, catalog no. AL0-8579).

The following reagents and buffers were used to perform the assay. The capture reagent was TGGAAAT-S1-BioTEG-3' (SAN-002485). The detection reagent was 5'-DIGC12-S1-GTAAAAGT (SAN-002486). The buffer 1 was 750 mM sodium chloride, 75 mM sodium citrate, and 0.05% (v/v) Tween-20 at pH 7.0. The buffer 2 was 750 mM sodium chloride, 75 mM sodium citrate, 35 nM capture reagent, 35 nM detection reagent, and 0.05% (v/v) Tween 20 at pH 7.0. The buffer 3 was 300 mM sodium chloride, 30 mM sodium citrate, and 0.05% (v/v) Tween 20 at pH 7.0.

The standard curve for the bioanalysis was made in the respective species plasma ranging from 5 to 5,000 nM, which was then 100-fold diluted with buffer 1 and then further 50-fold diluted with buffer 2, resulting in a 5,000-fold dilution affording a standard range from 1 to 1,000 pM. Prior to analysis, a minimum 10-fold dilution with buffer 2 was applied to all samples.

For pK analysis, a streptavidin-coated 96-well plate (Thermo Fisher Scientific, Waltham, MA, catalog no. 15119) was washed three times with buffer 1. A 100-μL volume of samples and standard curve were added and incubated for 60 min at room temperature. The plate was washed three times with buffer 3. The detection probe, anti-Dig-AP Fab fragment (Roche Applied Science, Penzberg, Germany, catalog no. 11 093274910) was added and incubated for 60 min at room temperature. The plate was washed three times with buffer 3. Last, Tropix CDP-Star Sapphire-II Substrate (Applied Biosystems, Foster City, CA, catalog no. T1025) was added and incubated for 30 min at room temperature. The ASO concentrations were measured by luminescence (Enspire, PerkinElmer, Waltham, MA).

Mouse PK/PD modeling
Data from C57Bl6/J mouse shown in Figure 4 were used for PK/PD modeling. The oligonucleotide was administered with ICV dosing and mice received only a single dose but at different levels, from 50 to 200 μg. The concentrations exponentially declined following the administration; therefore, a one-compartment PK model was used to fit the data.

The tau mRNA data were measured in the same studies and we found that the maxima knockdown was not immediate after ICV administration but a bit delayed. We therefore employed a turnover model to estimate both the potency of the compound and also the half-life of the tau mRNA. The same methodology was used to fit the tau protein. Inter-individual variability is not estimated since observations are available at only single time points per subject (destructive sampling). The residual error is therefore accounting for inter-individual variability, model misspecification, and other variability sources.

Cyno PK/PD modeling
For modeling out to 20 weeks post dose, PK and PD data from up to four studies and 25 monkeys were used, and the results are shown in

Figures 7 and S7. The oligonucleotide was administered with intrathecal dosing, and Cyno monkeys received two administrations 1 or 2 weeks apart at 8 mg. While the dose is administered directly in the CSF, the PK observations were made at the brain level in nine different regions. Therefore, similarly to the mice PK data, a one-compartment PK model was used to fit the data as if the dose was directly administered in the brain.

The first time point in the study was at 7 days post last injection, and potential delay in tau mRNA knockdown could not be observed. Tau mRNA knockdown was therefore fitted against the measured concentrations with a direct response model. A significant delay was observed for the knockdown of the protein, therefore a turnover model was used to fit the protein tau data.

Inter-individual variability is not estimated since observations are available at only single time points per subject (destructive sampling). The residual error is therefore accounting for inter-individual variability, model misspecification, and other variability sources.

PK/PD analysis software
Parameter estimation is performed using Monolix 2018R1 (Monolix software, analysis of mixed effects models, LIXOFT and INRIA, http://www.lixoft.com/) software using the linear approximation for the estimation of the Fisher information matrix. Simulations and figures were generated using RStudio Team (2020). RStudio: Integrated Development for R. RStudio, PBC, Boston, MA URL http://www.rstudio.com/.

Statistical analyses
Statistical analyses of mouse and monkey data were performed using Graphpad Prism v7.0. A one-way ANOVA followed by Dunnett's post hoc was used to test for treatment effects versus control. An RM ANOVA was conducted on time-course data presented followed by a Dunnett's post hoc analysis. Significance was set to $p < 0.05$.

Study approval
Mice and monkeys were maintained in accordance with the guidelines of the Animal Care and Use Committee of Bristol Myers Squibb (BMS), the "Guide for Care and Use of Laboratory Animals," and the guidelines published in the National Institutes of Health Guide for the Care and Use of Laboratory Animals. Animal experimental protocols and procedures were approved by the BMS Animal Care and Use Committee.

Data access
All the data are included in the main text or in the supplementary materials. RNA-seq data will be available on GEO.

DATA AVAILABILITY
The RNA-seq data reported in this study are deposited in the GEO database under the accession numbers GSE204930 and GSE204931.

SUPPLEMENTAL INFORMATION

ACKNOWLEDGMENTS

AUTHOR CONTRIBUTIONS

A.E. designed and analyzed mouse ASO studies. M.J. provided analysis and figures of cyno data. C.W., N.J.P., T.D., T.-H.O.Y., F.G., and R.J. designed experiments and tested ASOs in hESC and Cyno iPSCs for potency and off-target effects. P.H.H. designed ASO libraries. Y.Lu, A.F., and Y.Li. designed and ran Cyno ASO distribution and KD studies. J.M. provided pharmaceutics support. K.J., M.P., and G.C. conducted mouse dosing and observations tissue collection, and Tau ELISAs. J.N. conducted qPCR for mouse studies. M.W. designed Cyno ASO studies. M.W., J.P., and M.B. conducted Cyno studies in-life and sample collection. J.E.Meredith. and V.G. analyzed Cyno CSF Tau. L.H. and J.M.B. analyzed Cyno brain Tau. Y.B, A.B., and R.S. provided bioanalytical analyses and PK modeling. C.K. and M.G. conducted ASO screening in mouse Tau cortical neurons. J.L. provided safety assessments in Cyno. D.D. provided analytical PCO infrastructure. A.M.C. and C.F.A. conceptualized Tau ASO therapy and designed biology studies. S.E.M., R.E.O., and J.E.Macor. provided chemistry input and synthesis. A.M.H. designed and ran initial ASO screens. C.B. conducted PK/PD modeling. M.T. created graphic abstract, and generated and maintained human neuronal cultures.

DECLARATION OF INTERESTS

C.M.K., J.K.L., R.S., Y.B., D.D., S.E.M., and R.E.O. are employees of BMS and own stock or restricted stock units in BMS. A.E., Y. Li, Y. Lu, J.E. Meredith, J.E. Macor, M.W., V.W., K.J., M.G., J.M.B., L.H., A.F., J.P., M.B., A.B., J.E.M., C.F.A., and A.M.C. were employees of BMS when the work described was carried out. R.E.O., A.M.C., P.H.H., A.M.H., J.M.B., M.L.J., and S.E.M. are co-inventors on US Patent 10,799,523 and US patent applications US 2016/0237427, US 2018/0161356 and US 2019/0383797; and PCT patent application 2016/126995. P.H.H., R.E.O., A.M.H., and M.L.J. are co-inventors on US patent application US 2018/0023081.

REFERENCES

1. Weingarten, M.D., Lockwood, A.H., Hwo, S.Y., and Kirschner, M.W. (1975). A protein factor essential for microtubule assembly. Proc. Natl. Acad. Sci. USA 72, 1858–1862.

2. Chang, C.W., Shao, E., and Mucke, L. (2021). Tau: enabler of diverse brain disorders and target of rapidly evolving therapeutic strategies. Science 371, eabb8255.

3. Binder, L.I., Frankfurter, A., and Rebhun, L.I. (1985). The distribution of Tau in the mammalian central nervous system. J. Cell Biol. 101, 1371–1378.

4. LoPresti, P., Szuchet, S., Papasozomenos, S.C., Zinkowski, R.P., and Binder, L.I. (1995). Functional implications for the microtubule-associated protein tau: localization in oligodendrocytes. Proc. Natl. Acad. Sci. USA 92, 10369–10373.

5. Trushina, N.I., Bakota, L., Mulkidjanian, A.Y., and Brandt, R. (2019). The evolution of Tau phosphorylation and interactions. Front. Aging Neurosci. 11, 256.

6. Gendron, T.F., and Petrucelli, L. (2009). The role of tau in neurodegeneration. Mol. Neurodegener. 4, 13.

7. D'Souza, I., Poorkaj, P., Hong, M., Nochlin, D., Lee, V.M., Bird, T.D., and Schellenberg, G.D. (1999). Missense and silent tau gene mutations cause frontotemporal dementia with parkinsonism-chromosome 17 type, by affecting multiple alternative RNA splicing regulatory elements. Proc. Natl. Acad. Sci. USA 96, 5598–5603.

8. Poorkaj, P., Bird, T.D., Wijsman, E., Nemens, E., Garruto, R.M., Anderson, L., Andreadis, A., Wiederholt, W.C., Raskind, M., and Schellenberg, G.D. (1998). Tau is a candidate gene for chromosome 17 frontotemporal dementia. Ann. Neurol. 43, 815–825.

9. Stanford, P.M., Halliday, G.M., Brooks, W.S., Kwok, J.B., Storey, C.E., Creasey, H., Morris, J.G., Fulham, M.J., and Schofield, P.R. (2000). Progressive supranuclear palsy pathology caused by a novel silent mutation in exon 10 of the tau gene: expansion of the disease phenotype caused by tau gene mutations. Brain 123, 880–893.

10. Baker, M., Litvan, I., Houlden, H., Adamson, J., Dickson, D., Perez-Tur, J., Hardy, J., Lynch, T., Bigio, E., and Hutton, M. (1999). Association of an extended haplotype in the tau gene with progressive supranuclear palsy. Hum. Mol. Genet. 8, 711–715.

11. Braak, H., and Braak, E. (1991). Neuropathological staging of Alzheimer-related changes. Acta Neuropathol. 82, 239–259.

12. Leuzy, A., Chiotis, K., Lemoine, L., Gillberg, P.G., Almkvist, O., Rodriguez-Vieitez, E., and Nordberg, A. (2019). Tau PET imaging in neurodegenerative Tauopathies – still a challenge. Mol. Psychiatr. 24, 1112–1134.

13. Pooler, A.M., Polydoro, M., Maury, E.A., Nicholls, S.B., Reddy, S.M., Wegmann, S., William, C., Saqran, L., Cagsal-Getkin, O., Pitstick, R., et al. (2015). Amyloid accelerates tau propagation and toxicity in a model of early Alzheimer's disease. Acta Neuropathol. Commun. 3, 14.

14. Holmes, B.B., Furman, J.L., Mahan, T.E., Yamasaki, T.R., Mirbaha, H., Eades, W.C., Belaygorod, L., Cairns, N.J., Holtzman, D.M., and Diamond, M.I. (2014). Proteopathic tau seeding predicts tauopathy in vivo. Proc. Natl. Acad. Sci. USA 111, E4376–E4385.

15. DeVos, S.L., Corjuc, B.T., Oakley, D.H., Nobuhara, C.K., Bannon, R.N., Chase, A., Commins, C., Gonzalez, J.A., Dooley, P.M., Frosch, M.P., and Hyman, B.T. (2018). Synaptic tau seeding precedes tau pathology in human alzheimer's disease brain. Front. Neurosci. 12, 267.

16. He, Z., Guo, J.L., McBride, J.D., Narasimhan, S., Kim, H., Changolkar, L., Zhang, B., Gathagan, R.J., Yue, C., Dengler, C., et al. (2018). Amyloid-β plaques enhance Alzheimer's brain tau-seeded pathologies by facilitating neuritic plaque tau aggregation. Nat. Med. 24, 29–38.

17. Chalmers, K.A., and Love, S. (2007). Neurofibrillary tangles may interfere with Smad 2/3 signaling in neurons. J. Neuropathol. Exp. Neurol. 66, 158–167.

18. Hsieh, Y.-C., Guo, C., Yalamanchili, H.K., Abreha, M., Al-Ouran, R., Li, Y., Dammer, E.B., Lah, J.J., Levey, A.I., Bennett, D.A., et al. (2019). Tau-mediated disruption of the spliceosome triggers cryptic RNA splicing and neurodegeneration in Alzheimer's disease. Cell Rep. 29, 301–316.e10.

19. Congdon, E.E., and Sigurdsson, E.M. (2018). Tau-targeting therapies for Alzheimer disease. Nat. Rev. Neurol. 14, 399–415.

20. Mignon, L., Kordasiewicz, H., Lane, R., Smith, A., Miller, T., Narayanan, P., Swayze, E.E., Norris, D., Fitzsimmons, B., and Bennett, F. (2018). Design of the first-in-human study of IONIS-MAPTRx, a tau-lowering antisense oligonucleotide, in patients with alzheimer disease. Neurology 90. 006.

21. DeVos, S.L., Goncharoff, D.K., Chen, G., Kebodeaux, C.S., Yamada, K., Stewart, F.R., Schuler, D.R., Maloney, S.E., Wozniak, D.F., Rigo, F., et al. (2013). Antisense reduction of tau in adult mice protects against seizures. J. Neurosci. 33, 12887–12897.

22. DeVos, S.L., Miller, R.L., Schoch, K.M., Holmes, B.B., Kebodeaux, C.S., Wegener, A.J., Chen, G., Shen, T., Tran, H., Nichols, B., et al. (2017). Tau reduction prevents

neuronal loss and reverses pathological tau deposition and seeding in mice with tauopathy. Sci. Transl. Med. 9, eaag0481.

23. Vester, B., and Wengel, J. (2004). LNA (locked nucleic acid): high-affinity targeting of complementary RNA and DNA. Biochemistry 43, 13233–13241.

24. Kordasiewicz, H.B., Stanek, L.M., Wancewicz, E.V., Mazur, C., McAlonis, M.M., Pytel, K.A., Artates, J.W., Weiss, A., Cheng, S.H., Shihabuddin, L.S., et al. (2012). Sustained therapeutic reversal of Huntington's disease by transient repression of huntingtin synthesis. Neuron 74, 1031–1044.

25. McCampbell, A., Cole, T., Wegener, A.J., Tomassy, G.S., Setnicka, A., Farley, B.J., Schoch, K.M., Hoye, M.L., Shabsovich, M., Sun, L., et al. (2018). Antisense oligonucleotides extend survival and reverse decrement in muscle response in ALS models. J. Clin. Invest. 128, 3558–3567.

26. Polydoro, M., Acker, C.M., Duff, K., Castillo, P.E., and Davies, P. (2009). Age-dependent impairment of cognitive and synaptic function in the hTau mouse model of tau pathology. J. Neurosci. 29, 10741–10749.

27. Hagedorn, P.H., Brown, J.M., Easton, A., Pierdomenico, M., Jones, K., Olson, R.E., Mercer, S.E., Li, D., Loy, J., Høg, A.M., et al. (2022). Acute neurotoxicity of antisense oligonucleotides after intracerebroventricular injection into mouse brain can Be predicted from sequence features. Nucleic Acid Therapeut. 32, 151–162. https://doi.org/10.1089/nat.2021.0071.

28. Goedert, M., Spillantini, M.G., Jakes, R., Rutherford, D., and Crowther, R.A. (1989). Multiple isoforms of human microtubule-associated protein tau: sequences and localization in neurofibrillary tangles of Alzheimer's disease. Neuron 3, 519–526.

29. Hagedorn, P.H., Pontoppidan, M., Bisgaard, T.S., Berrera, M., Dieckmann, A., Ebeling, M., Møller, M.R., Hudlebusch, H., Jensen, M.L., Hansen, H.F., et al. (2018). Identifying and avoiding off-target effects of RNase H-dependent antisense oligonucleotides in mice. Nucleic Acids Res. 46, 5366–5380.

30. Kuespert, S., Heydn, R., Peters, S., Wirkert, E., Meyer, A.L., Siebörger, M., Johannesen, S., Aigner, L., Bogdahn, U., and Bruun, T.H. (2020). Antisense oligonucleotide in LNA-gapmer design targeting TGFBR2 – a key single gene target for safe and effective inhibition of TGFβ signaling. Int. J. Mol. Sci. 21, 1952.

31. Irwin, S. (1968). Comprehensive observational assessment: a systematic quantitative procedure for assessing the behavioral and physiological state of the mouse. Psychopharmacologia 13, 222–257.

32. Sato, C., Barthélemy, N.R., Mawuenyega, K.G., Patterson, B.W., Gordon, B.A., Jockel-Balsarotti, J., Sullivan, M., Crisp, M.J., Kasten, T., Kirmess, K.M., et al. (2018). Tau kinetics in neurons and the human central nervous system. Neuron 98, 861–864.

33. Duff, K., Knight, H., Refolo, L.M., Sanders, S., Yu, X., Picciano, M., Malester, B., Hutton, M., Adamson, J., Goedert, M., et al. (2000). Characterization of pathology in transgenic mice over-expressing human genomic and cDNA tau transgenes. Neurobiol. Dis. 7, 87–98.

34. Santacruz, K., Lewis, J., Spires, T., Paulson, J., Kotilinek, L., Ingelsson, M., Guimaraes, A., DeTure, M., Ramsden, M., McGowan, E., et al. (2005). Tau suppression in a neurodegenerative mouse model improves memory function. Science 309, 476–481.

35. Blackmore, T., Meftah, S., Murray, T.K., Craig, P.J., Blockeel, A., Phillips, K., Eastwood, B., O'Neill, M.J., Marston, H., Ahmed, Z., et al. (2017). Tracking progressive pathological and functional decline in the rTg4510 mouse model of tauopathy. Alzheimer's Res. Ther. 9, 77.

36. Roberson, E.D., Scearce-Levie, K., Palop, J.J., Yan, F., Cheng, I.H., Wu, T., Gerstein, H., Yu, G.Q., and Mucke, L. (2007). Reducing endogenous tau ameliorates amyloid beta-induced deficits in an Alzheimer's disease mouse model. Science 316, 750–754.

37. Roberson, E.D., Halabisky, B., Yoo, J.W., Yao, J., Chin, J., Yan, F., Wu, T., Hamto, P., Devidze, N., Yu, G.Q., et al. (2011). Amyloid-β/Fyn-induced synaptic, network, and cognitive impairments depend on tau levels in multiple mouse models of Alzheimer's disease. J. Neurosci. 31, 700–711.

38. Ittner, L.M., Ke, Y.D., Delerue, F., Bi, M., Gladbach, A., van Eersel, J., Wölfing, H., Chieng, B.C., Christie, M.J., Napier, I.A., et al. (2010). Dendritic function of tau mediates amyloid-beta toxicity in Alzheimer's disease mouse models. Cell 142, 387–397.

39. Gheyara, A.L., Ponnusamy, R., Djukic, B., Craft, R.J., Ho, K., Guo, W., Finucane, M.M., Sanchez, P.E., and Mucke, L. (2014). Tau reduction prevents disease in a mouse model of Dravet syndrome. Ann. Neurol. 76, 443–456.

40. Djukic, B. (2016). Efficacy of tau antisense oligonucleotides in a mouse model of genetically determined epilepsy. In Paper Presented at: The Society for Neuroscience. Nov 12-16, San Diego, CA, USA.

41. Cacace, A. (2016). Discovery of tau antisense oligonucleotides for the treatment of tauopathy and epilepsy disorders. In Paper Presented at: The Society for Neuroscience. Nov 12-16, San Diego, CA, USA.

42. Jafar-nejad, P., Powers, B., Soriano, A., Zhao, H., Norris, D.A., Matson, J., DeBrosse-Serra, B., Watson, J., Narayanan, P., Chun, S.J., et al. (2021). The atlas of RNase H antisense oligonucleotide distribution and activity in the CNS of rodents and non-human primates following central administration. Nucleic Acids Res. 49, 657–673.

43. Roberts, T.C., Langer, R., and Wood, M.J.A. (2020). Advances in oligonucleotide drug delivery. Nat. Rev. Drug Discov. 19, 673–694.

44. Barten, D.M., Cadelina, G.W., and Weed, M.R. (2017). Dosing, collection, and quality control issues in cerebrospinal fluid research using animal models. Handb. Clin. Neurol. 146, 47–64.

45. van Poelgeest, E.P., Swart, R.M., Betjes, M.G.H., Moerland, M., Weening, J.J., Tessier, Y., Hodges, M.R., Levin, A.A., and Burggraaf, J. (2013). Acute kidney injury during therapy with an antisense oligonucleotide directed against PCSK9. Am. J. Kidney Dis. 62, 796–800.

46. Morris, M., Hamto, P., Adame, A., Devidze, N., Masliah, E., and Mucke, L. (2013). Age-appropriate cognition and subtle dopamine-independent motor deficits in aged tau knockout mice. Neurobiol. Aging 34, 1523–1529.

47. Lei, P., Ayton, S., Moon, S., Zhang, Q., Volitakis, I., Finkelstein, D.I., and Bush, A.I. (2014). Motor and cognitive deficits in aged tau knockout mice in two background strains. Mol. Neurodegener. 9, 29.

48. Gonçalves, R.A., Wijesekara, N., Fraser, P.E., and De Felice, F.G. (2020). Behavioral abnormalities in knockout and humanized tau mice. Front. Endocrinol. 11, 124.

49. Kimura, T., Whitcomb, D.J., Jo, J., Regan, P., Piers, T., Heo, S., Brown, C., Hashikawa, T., Murayama, M., Seok, H., et al. (2013). Microtubule-associated protein tau is essential for long-term depression in the hippocampus. Philos. Trans. R. Soc. Lond. B Biol. Sci. 369, 20130144.

50. Marciniak, E., Leboucher, A., Caron, E., Ahmed, T., Tailleux, A., Dumont, J., Issad, T., Gerhardt, E., Pagesy, P., Vileno, M., et al. (2017). Tau deletion promotes brain insulin resistance. J. Exp. Med. 214, 2257–2269.

51. Vallés-Saiz, L., Peinado-Cahuchola, R., Ávila, J., and Hernández, F. (2022). Microtubule-associated protein tau in murine kidney: role in podocyte architecture. Cell. Mol. Life Sci. 79, 97.

52. van Hummel, A., Bi, M., Ippati, S., van der Hoven, J., Volkerling, A., Lee, W.S., Tan, D.C.S., Bongers, A., Ittner, A., Ke, Y.D., and Ittner, L.M. (2016). No overt deficits in aged tau-deficient C57Bl/6.Mapttm1(EGFP)kit GFP knockin mice. PLoS One 11, e0163236.

53. Kaufman, S.K., Sanders, D.W., Thomas, T.L., Ruchinskas, A.J., Vaquer-Alicea, J., Sharma, A.M., Miller, T.M., and Diamond, M.I. (2016). Tau prion strains dictate patterns of cell pathology, progression rate, and regional vulnerability in vivo. Neuron 92, 796–812.

54. Scheres, S.H., Zhang, W., Falcon, B., and Goedert, M. (2020). Cryo-EM structures of tau filaments. Curr. Opin. Struct. Biol. 64, 17–25.

55. Goedert, M., and Spillantini, M.G. (2019). Ordered assembly of tau protein and neurodegeneration. In Tau Biology, Advances in Experimental Medicine and Biology, 1184, A. Takashima, B. Wolozin, and L. Buee, eds (Springer), pp. 3–21.

56. Dujardin, S., Commins, C., Lathuiliere, A., Beerepoot, P., Fernandes, A.R., Kamath, T.V., de los Santos, M.B., Klickstein, N., Corjuc, D.L., Corjuc, B.T., et al. (2020). Tau molecular diversity contributes to clinical heterogeneity in Alzheimer's disease. Nat. Med. 26, 1256–1263.

57. Love, M.I., Huber, W., and Anders, S. (2014). Moderated estimation of fold change and dispersion for RNA-seq data with DESeq2. Genome Biol. 15, 550.

58. Haley, T.J., and McCormick, W.G. (1957). Pharmacological effects produced by intracerebral injection of drugs in the conscious mouse. Br. J. Pharmacol. Chemother. 12, 12–15.